The nuclear localization and stability of the MITF transcription factor

Sigurður Rúnar Guðmundsson

Ritgerð til meistaragráðu
Háskóli Íslands
Læknadeild
Heilbrigðisvísindasvið

HÁSKÓLI ÍSLANDS

Kjarnstaðsetning og stöðugleiki umritunarþáttarins MITF

Sigurður Rúnar Guðmundsson

Ritgerð til meistaragráðu í líf og læknisfræði

Umsjónarkennarar: Eiríkur Steingrímsson

Leiðbeinandi Margrét Helga Ögmundsdóttir

Aðrir í meistaranáms nefnd:

Valerie Helene Maier

Læknadeild

Heilbrigðisvísindasvið Háskóla Íslands

Apríl 2015

The nuclear localization and stability of the MITF transcription factor

Sigurður Rúnar Guðmundsson

Thesis for the degree of Master of Science

Supervisors: Eirikur Steingrímsson & Margrét Helga Ögmundsdóttir

Other Masters Committee members:

Valerie Helene Maier

Faculty of Medicine

School of Health Sciences

April 2015

Prentun: Háskólaprent

Reykjavík, Ísland 2015

Ágrip

Umritunarþátturinn MITF (Microphthalmia-associated transcription factor) stjórnar þroskun og sérhæfingu litfruma og er mikilvægur áhættuþáttur í myndun sortuæxla (melanoma). Þótt MITF sé að mestu leyti staðsett í kjarna lit- og sortuæxlisfruma þá er lítið vitað um það hvernig staðsetningu þess er stjórnað í þessum frumum. Í þessu verkefni kortleggjum við hvaða svæði MITF próteinsins hafa áhrif á kjarnstaðsetningu próteinsins. Einnig skoðum við hvaða svæði próteinsins hafa áhrif á stöðuleika þess.

Til að gera þetta var útbúin genaferja sem tjáir EGFP-MITF samrunaprótein og stökkbreytingar útbúnar sem breyta tilteknum hlutum MITF próteinsins. Genaferjunni var komið fyrir í bæði 501Mel sortuæxlisfrumum og í HEK 293T frumum og staðsetning stökkbreyttu próteinanna í frumunum borin saman við staðsetningu villigerðar-MITF. Staðsetning og stöðuleiki próteinsins var ákvarðað með lagsjá (confocal microscope) og Western blot greiningu, með og án sérhæfðra hindra.

Niðurstöðurnar sýna að merki um staðsetningu í kjarna er staðsett í basíska hneppi (basic domain) MITF próteinsins. Þar sem stökkbreytt MITF án basíska hneppisins kemst inn í kjarna teljum við líklegt að önnur svæði í MITF hafi einnig áhrif á staðsetningu próteinsins í kjarna. Hvorki er þörf á DNA bindingu né tvenndarmyndun til þess að MITF próteinið haldist inn í kjarna. Við sýnum líka að MITF er að hluta til brotið niður með sjálfsáti og að svæði í carboxyl-enda próteinsins er mikilvægt fyrir þetta ferli.

Við höfum því staðsett kjarna-merki í MITF og sýnum að próteinið er brotið niður með sjálfsáti.

Abstract

MITF (Microphthalmia-associated transcription factor) regulates development and differentiation of melanocytes and is a key component in formation of melanoma. Although MITF is primarily nuclear in melanocytes and melanoma cells, little is known about how sub-cellular localization of MITF is regulated in these cells. In this project we characterize which domains of the MITF protein are involved in determining nuclear localization and protein stability.

We generated EGFP-MITF fusion constructs carrying wild-type and mutant versions of MITF and transfected into human 501Mel (melanoma) and HEK 293T (embryonic kidney) cells to map which domains of MITF are involved in nuclear localization and protein stability. The subcellular location and stability of MITF were determined using a confocal microscope and western analysis with or without pathway-specific inhibitors.

We observed that a monopartite nuclear localization signal is located in the basic domain of MITF and is required for the nuclear localization of MITF. However, since a MITF protein lacking the entire basic domain is still able to enter the nucleus, it is likely that other regions also impact on nuclear localization. Neither DNA binding nor dimerization are necessary for nuclear retention of MITF. We also showed that MITF is degraded at least partly through the autophagosomal pathway.

We have localized the major nuclear localization signal in MITF and shown that the protein is degraded through the autophagosomal pathway**.**

Acknowledgements

This thesis was carried out in the department of biochemistry and molecular biology in the faculty of medicine. Many people have supported me and helped me directly or indirectly and I would like to thank them all for their kindness and support.

I would like to start by thanking **Professor Eiríkur Steingrímsson** for giving me the opportunity to do my thesis work in his group. It has been an inspiration to be a part of Eiríkur's group for the last couple of years and his dedication and excitement over new results affect everybody around him in a positive way. I am very grateful for the opportunity of being allowed to grow as an independent scientist and not only work independently on experiments but to have been a part of shaping the progress of my thesis.

I would like to thank **Dr Margrét Helga Ögmundsdóttir** for her supervision and for all her help in designing and setting up experiments, and her patience for unrelenting questions and comments. I also want to thank both **Eiríkur** and **Margrét** for all the help preparing this thesis, and I would like to thank **Valerie Helene Maier** for her contributions in my masters committee.

I want to thank **Kristín Bergsteinsdóttir** for all her help and instructions during my time at the lab.

I would also like to thank all the other people involved in this project **Sandra Diebel, Josué Ballesteros, Indriði Einar Reynisson and Alexander Schepsky.** It has been a privilege to work with these scientists towards a common goal. Furthermore I would like to thank my fellow student at Eiríkur's lab. **Remina Dilixiati, Kimberley Anderson, Katrín Möller, Sandra Diebel, Josué Ballesteros, Diahann Atacho** and **Kristján Hólm Grétarsson** for all their help, support and all the critical and nerdy discussions we have had and I hope we will continue to collaborate in the future. I also want to thank **Margrét Bessadóttir** for her input and I want to specially thank **Sævar Ingþórsson** for all his help imaging these constructs and for all the helpful comments, advice on imaging and all things biological.

Last but certainly not the least I want to thank my family for all their support, I specially want to thank my parents **Guðmundur** and **Sigríður** for their help and support through the years to get to where I am. I also want to thank my loving girlfriend **Selma Rut** who's support and encouragement got me through the tough times and still is willing to listen to me prepare presentations or proof read my documents .

Finally I want to dedicate this thesis to my grandparents

Ingibjörg Ástvaldsdóttir and Hjörleifur Gunnarsson.

From the bottom of my heart, thank you all

Table of content

List of figures

List of tables

List of abbreviations

a.a.: Amino Acid

ARM repeats: Armadillo repeats

BSA: Bovine Serum Albumin

C-FOS: Proto-oncogene c-Fos

CHX: Cyclohexamide

CQ: Chloroquine

CRM1: chromosomal maintenance 1 / Exportin 1

DAPI: 4',6-diamidino-2-phenyl-indole

DMEM: Dulbecco's Modified Eagle Medium

EGFP: Enhanced Green Fluorescent Protein

FBS: Fetal Bovine Serum

GTP/GDP: Guanosine triphosphate driphosphate / Guanosine diphosphate

HEAT repeats: Huntingtin, elongation factor repeats

IBB Importin Beta binding domain

IBB: Importin β binding domain

kDa: Kilo Dalton

LAMP2: Lysosome-Associated Membrane Protein 2

LC3: Microtubule-associated protein 1A/1B-light chain 3

LTB gel: Lower Tris Buffer

M132: Carbobenzoxy-Leu-Leu-leucinal

MAX: Myc-Associated factor X

MITF: Microphthalmia-Associated Transcription Factor.

mTORC1: Mechanistic Target Of Rapamycin Complex 1

MYC: Myc proto-oncogene protein

NES: Nuclear Export Signal

NGS: Normal Goat Serum

NLS: Nuclear Localization Signal.

NPC: Nucleopore complex

Nups: Nucleoporins

PBS: Phosphate-buffered saline

PMFS: Phenylmethanesulfonyl fluoride

PTMT Post translational modification

Pu 1 31 kDa-transforming protein / Transcription factor PU.1

RCC1: Regulator of chromosome condensation 1

RIPA buffer: Radio-Immuno-precipitation Assay Buffer

SDS: Sodium Dodecyl Sulfate

SILV: Silver locus protein homolog

TFE3: Transcription factor E3

TFEB: Transcription factor EB

TFEC: Transcription factor EC

USF: Upstream stimulatory factor

UTB gel: Upper Tris Buffer

1 Introduction

1.1 The Microphthalmia-associated transcription factor

In 1942 Paula Hertwig published results where she described white, small-eyed mice. She named the mutation resulting in this phenotype microphthalmia (5). Exactly fifty years later, in 1992, the MITF gene was first identified as a B/hlh/Z transcription factor termed MITF (microphthalmia associated transcription factor) (5). And now, 73 years after Hertwig's paper was published, MITF is recognized as a master regulator of melanocytes and a critical survival factor in melanoma. This single gene is now known to play multiple vital roles in the body. MITF mutations have been shown to cause loss of pigmentation, reduced eye size and blindness. Lack of proper MITF function also leads to deafness, causes a lower mast cell count and affects osteoclasts such that they are not able to perform secondary bone absorption (6). MITF is closely related to TFEB and TFE3 and can either form a homodimer by itself or heterodimer with either TF3B or TFE3. Interestingly, MITF cannot heterodimerize with other B/hlh/z transcription factors such as MYC, MAX and USF (6).

MITF is now known to have multiple isoforms (7, 8) called A,J,C,E,H,D,B,M,CX, caused by alternative splicing and different cell specific promoters. In this thesis we will focus on the nuclear localization and protein stability of the MITF-M isoform in melanoma cells. All of MITF's isoforms share the region encoded by exon 2-9 and the variability between isoforms lies with their different N termini which vary in both length and sequence (9). MITF-M is known as the melanoma and melanocytic specific isoform. However, MITF-M is also found in mast cells and in the heart (10). MITF-M is the shortest of the MITF isoforms and is comprised of 419 amino acids (11).

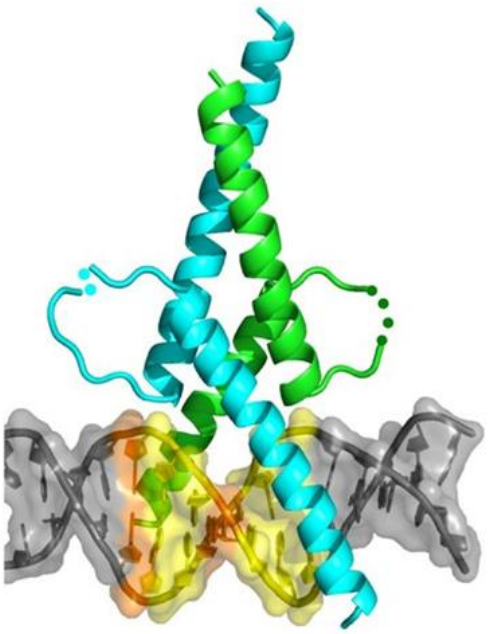

Figure 1. Structural model of the MITF binding and assembly domain. The image is copied and adapted from Pogenberg et al. 2012 (1).

A number of mutations are known in MITF in both humans and mice (12). The known MITF mutations can be categorized into 2 subgroups. The first group consists of mutations that interfere with MITF's ability to bind to DNA. MITF recognises both E-box (CACGTG) and M-box (TCATGTG) promoter sequences. MITF target genes showed that 11 of 18 mutation correlating with Waardenburg and Tiez syndromes fail to bind DNA. 6 of these 11 mutations are in the DNA binding domain (214-217). Interestingly mutations located in the helix–loop-helix and zipper domains also affect DNA binding (12). The second group is comprised of mutations in domains of unknown function, or mutations which affect post translational modification (PTM) of MITF. These include the mutations E87R, L135V, L142F, E318K, D380N, all of which were first discovered in melanomas (12). Most prominent of these is the germline E318K mutation, found in melanoma families, where the glutamate amino acid at position 318 is mutated to lysine. This mutation disrupts SUMOylation of a.a. 316, increasing MITF's stability and binding to subset of target genes resulting in an altered gene expression pattern. The E318K mutation is a germline mutation that is known to increase melanoma risk fivefold as well as increase risk of renal carcinoma (13).

Gene amplification can be found in 20% of all metastatic melanomas. Tumour gene amplification can cause a copy number increase to an average of 4 – 12 copies. Melanoma patients on BRAF/MEK inhibitors have shown MITF gene amplification, hinting at a potential role in melanoma drug resistance (14). Little is known about the nuclear localization of MITF. One paper suggested that Exon1B1b might play a role in retaining MITF in the cytoplasm, and that MITF-M's lack of the 1B1b exon is responsible for the higher transcription activity and nuclear concentration of MITF-M over the other isoforms (9). Another paper suggested that the $MITF^{mi}$ mutation at MITF, which deletes one arginine in the DNA binding domain of MITF, leads to effects on nuclear localization (15). Homozygous mice carrying the $MITF^{mi}$ mutation have a white coat colour and lack melanocytes. In addition Mi mutations in mice has been shown to be able to affect nuclear localization of the transcription factors Pu.1 and c-Fos, contributing to osteopetrosis (16).

1.2 Nuclear Localization Signals

Nuclear Localization Signals (NLS) are categorized into two groups: classical NLS or non-classical NLS. Classical NLS are a short motif of positively charged lysines or arginines (17). These motifs are either monopartite or bipartite. Bipartite NLS have 2 short motifs of lysines or arginines divided by a spacer of about 10 amino acids (a.a.). Proteins with classical NLS bind to Importin α family members that actually have a bipartite NLS specific to Importin α1. This trimeric complex is then able to move through the nucleopore (18). Non classical NLS is a receptor like motif that can bind directly to Importin β and initiate the import mechanism.

There are 3 distinct ways. Importin α proteins actually use classical like NLS to bind to Importin β1, while the C-termini of α1 binds to a cargo protein (2), the N-termini use the same mechanism to bind to Importin β. The second binding mechanism involve cargo proteins containing PY NLS (R/K/H-X(2–5)-P-Y where X is any residue) proteins containing these proline-tyrosine dipeptide in their C-termini can bind to Importin β2 to enable non classical nuclear localization (18). Finally the third transport method involves Exportin 1 (CRM1) that binds cargo proteins that contain a leucine rich nuclear export signal(NES) (18).

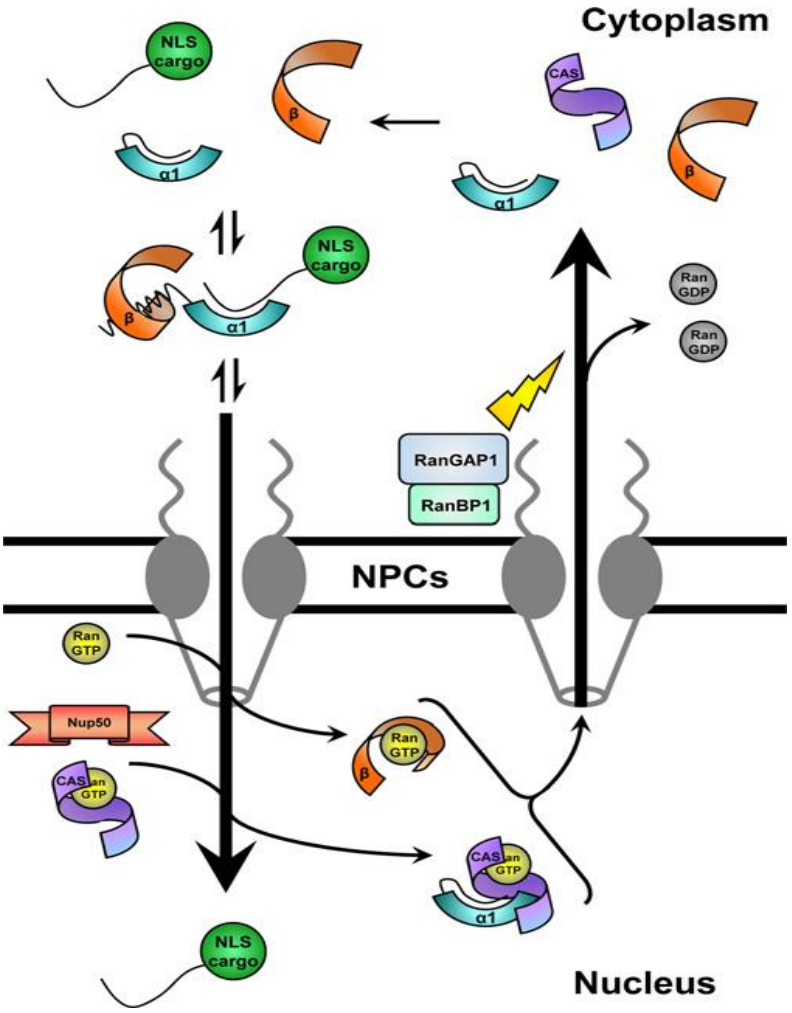

Figure 2. Importin mediated nuclear transport. A schematic view of Importin mediated transport through the nucleopore complex. Figure is copied and adapted from Pumroy et al. 2015 (2).

1.2.1 Importin α the protein adaptor

Proteins that have classical NLS can bind to one of the members of the Importin α protein family (2). Importin α proteins essentially act as adaptor molecules. They cannot import cargo proteins by themselves into the nucleus but can bind to both cargo proteins and Importin β and mediate nuclear import (2).

All Importin α proteins have fundamentally similar protein structure. An N-terminal, auto-inhibitory, Importin-β-binding (IBB) domain and a C-termini comprised of ten armadillo (ARM) repeats are wound

up and make up the core of the protein which binds to NLS on cargo proteins. A simplistic way of thinking about the structure and function of Importin α is to think of a hairpin where the IBB domain is inhibited by the ARM repeats. When a cargo protein binds to the ARM repeats the IBB domain is activated and can bind to Importin β imitating nuclear import. A weak binding potential between Importin α and a NLS sequence of a cargo protein sometimes needs to be in the proximity of Importin β so the interaction can occur. This inhibition of the IBB domain excludes any possibility of Importin α transferring to the nucleus without a cargo protein (2).

In humans there are 7 subtypes of Importin α (α1, α3, α4, α5, α6, α7 and α8) that are divided into 3 subfamilies. *Saccharomyces cerevisiae* has one orthologue of Importin β (no Importin α) and *Drosophila melanogaster* has 3 orthologues of Importin α. This increase of Importin α subtypes is an evolutionary additive that enables more complex cell specificity. Despite the high similarity between Importin α subtypes there is high specificity in vivo (2).

1.2.2 The transport protein Importin β

The Importin β family is a big group of Importins, Exportins and bidirectional receptors. There are 10 Importins (Importin-β1, β2, β2b2, β3 Importin-4, 7, 8, 9, 11, 12), 7 Exportins (Exportin-1, 2, 5, 6, 7, t and RanBP17). Then there are 2 bidirectional receptors (Importin 13 and Exportin 4). Finally there is RanBP6 that has not been characterized as carefully as the other proteins (18).

Structural similarity between Importin β proteins is low (lower than 20% a.a. identity). This variance is also seen in different protein size that can vary from 90-130 kDa (19). The highest a.a. sequence similarity is in the N- termini of the proteins that incidentally contains the Ran GTP binding site. The C-termini of the proteins holds the cargo protein binding site, and its a.a. sequence variability explains diverse functions of the Importin β family members. Importin β proteins contain 19 or 20 HEAT repeats that make the protein flexible. This flexibility enables the Ran GTP/GDP to alter the protein conformation, thus enabling some Importin β proteins to bind or release their cargo units (20).

The subcellular location of RCC1, Ran GAP1 and Ran BP1 is the foundation of the direction of nuclear transport. This is evident when we look at the mainly nuclear RCC1 complex that phosphorylates Ran GDP to Ran GTP and the cytoplasmic Ran GAP1 and its co-factor Ran BP1 that converts Ran GTP to Ran GDP (18). Importin β proteins that are responsible for nuclear import bind their cargo, including Importin α in the cytoplasm and are then able to translocate into the nucleus. In the nucleus Ran GTP binds to the Importin-cargo complex causing a conformational change, releasing the cargo. The Importin-Ran GTP complex is then transported out of the nucleus where Ran GAP1 and Ran BP1 hydrolyse Ran GTP to Ran GDP causing conformational change, releasing Ran GTP. For Exportin 1 the story is reversed. In the nucleus Exportin 1, the cargo to be exported and Ran GTP bind in a trimeric complex that is transported through the nucleopore complex to the cytoplasm.

In the cytoplasm Ran GTP is converted into Ran GDP causing the cargo to be released. When back in the nucleus, RCC1 phosphorylates Ran GDP to Ran GTP leading to either binding to another cargo unit or releasing Ran GTP from Exportin 1 (18).

1.3 The Nucleopore Complex

The Nuclear envelope is studded with Nucleopore complexes (NPC), cellular megastructures approximately 50 MDa in size and composed of ~30 different proteins named nucleoporins (Nups) (21). The NPC is a circular structure with a central tube. On the cytoplasmic side there are characteristic 8 spokes and a basket on the nuclear side. Proteins smaller than ~40 kDa can passively diffuse through the NPC but larger complexes have to be actively transported through the membrane with the help of Importins or Exportins. FG Nups are proteins with long sequence repeats of phenylalanine and glycine. The FG Nups are located both on the spokes in the cytoplasm enabling the spokes to direct proteins to and from specific regions of the cell and in the central tube of the NPC allowing transport of proteins through the actual nuclear envelope. Nuclear transport receptors such as Importins can bind to these Nups with low affinity, and these binding events seem to occur sequentially to move the Importin and its cargo towards and trough the nucleopore (21).

1.4 Autophagy mediated degradation of proteins

Autophagy is one of the cellular reactions to stress situations such as starvation and oxidative stress and has also been suggested to degrade intracellular microbes (3). Autophagy is a broad term for 3 related degradation pathways (3). These are: chaperone mediated autophagy, micro autophagy and macro autophagy. Here we will only discuss macro autophagy (here after called autophagy). In addition to cell stress responses, autophagy is also responsible for degradation of misfolded proteins and as a regulator of protein turnover in healthy proteins (22). Autophagy has been shown to have a dual role in cancer. Based on mouse studies, it is believed to inhibit cells turning cancerous by removing cellular debris. However it also increases cell survival and growth in established tumours by the same mechanism (23). Dysregulation of the clearance of protein aggregates by autophagy has also been shown to lead to neurodegenerative diseases such as Parkinson's disease. Autophagy is a complex process and can be split up into 5 steps (3).

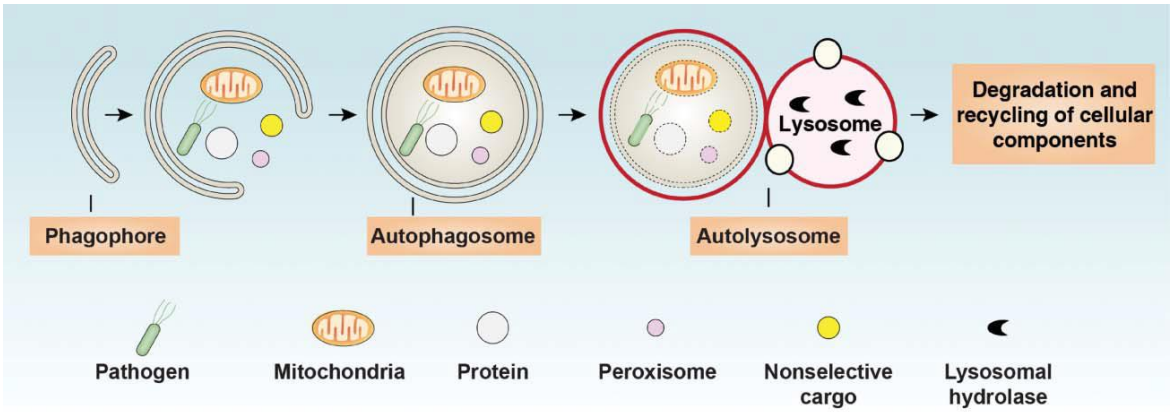

Figure 3. Schematic representation of the complex mechanism of autophagy. Figure copied from Xie et al. 2015 (3).

1. The best characterized regulator of autophagy induction is the mechanistic target of rapamycin complex 1 (mTORC1). It is active in the presence of amino acids and inhibits the autophagy process. This regulation by mTORC1 is not only via direct phosphorylation of proteins required for the autophagy process, but also at the level of transcriptional regulation. MTORC1 phosphorylates the transcription factor TFEB which results in it being retained in the cytoplasm (23-25). When mTORC1 becomes inactive in response to amino acid starvation, TFEB is no longer phosphorylated and enters the nucleus where it promotes the transcription of autophagy genes. The same shuttling mechanism has been shown for the long MITF isoform. However, MITF-M lacks the N-terminal mTORC1 interaction site and is present in the nucleus in the presence of nutrients. Indeed, autophagy is high in melanoma cells and unpublished data in our lab shows that MITF-M regulates autophagy genes and is important for the autophagy process in these cells.

2. During nucleation the phagophore proteins such as p62 and NBR1 (neighbour of BRC1 protein1) are recruited to ubiqutinated proteins destined for degradation. The binding of these proteins induce the recruitment of lipids and proteins to the phagophore. PtdIns3K (class III phosphatidylinositol 3-kinase complex) then plays a complex role in formation of the autophagosome.

3. Immediately after nucleation the Elongation step begins where the E2 ligase starts to ubiquitinate the substrate and then the E1 and E3 ligases along with p62 and LC3 start the elongation of the double membrane forming the autophagosome.

4. After the formation of the autophagosome it is moved along the microtubules in a dynein-dependent manner (3). The microtubules lead the autophagosome to the microtubule organizing center near the nucleus where the lysosome is located. There the SNARE (soluble NSF [N-ethyl-maleimide- soluble NSF [N-ethyl-maleimide-sensitive fusion protein] attachment protein receptor sensitive fusion Protein) protein family is responsible for the fusion of a lysosome and autophagosome, producing an autolysosome.

5. Autophagy is not considered complete until the cargo has been degraded and the macromolecules released back into the cytoplasm. This step relies on many hydrolases and the low pH of the autolysosome for degradation and efficient membrane transporters for the recycling of the macromolecules.

1.5 Proteasomal degradation pathway.

The proteasomal degradation pathway has been described as the cell's main degradation pathway, degrading 80-90% of the cellular proteins (4). The proteasome (26S proteasome) is a large cellular structure that is comprised of mainly 2 subunits. The 20S core is the core unit of the proteasome and is the subunit that actually unfolds and disassembles the degradation proteins into short a.a. sequences that can either be reused or degraded further. This elongated tubular unit of the proteasome is narrowed on each end suggesting that proteins need to be partially unfolded to enter the 20S core of the proteasome (26).

The other subunit of the proteasome is the 19S subunit, located at each end of the 20S core complex. The 19S unit is responsible for binding ubiquitinated proteins and enable their degradation while inhibiting degradation of un-ubiquitinated proteins. 19S subunit also removes the ubiquitination from degrading proteins (26). The 11S subunit has been reported to interact in some cases with the 19S complex and thus enable the proteasome to degrade foreign proteins such as viral proteins, but this is not in the scope of this thesis.

1.6 Ubiquitination of proteins

Protein ubiquitination is an emerging field. Among the roles for ubiquitination are proteosomal or autophagosomal degradation, post transcriptional modification or intracellular signalling. Ubiquitination is a three step process involving 3 different enzymes (4). The first step is activation of the E1 ubiquitin activation enzyme. Next is the conjugation where the ubiquitin and the E1 enzyme are bound to the E2 ubiquitin enzyme and finally the E1 enzyme is released. The third and final step is when the E3 ubiquitin ligase catalyses the binding of ubiquitin to a lysine a.a. on the protein to be ubiquitinated causing the E2 enzyme to release and finishing the process (27).

There are 3 different types of ubiquitination labelling of proteins: Mono ubiquitination where a single ubiquitin molecule is attached to the substrate; Multi mono-ubiquitination where multiple ubiquitin molecules are attached to different lysines on the substrate and poly ubiquitination where a chain of 7 ubiquitins are attached to the lysine on the substrate. To further increase the diversity of ubiquitin labelling, poly-ubiquitin chains can either be uniform by linking to each other using lysine 48 or 63 binding or produce atypical branching chains by linking through lysines 6, 27 or 48 (27).

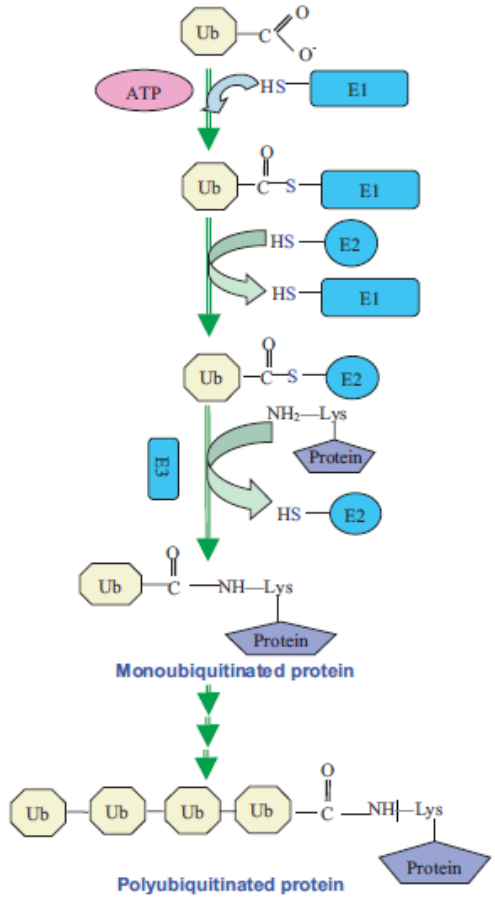

Figure 4. The 3 steps of ubiquitination. A schematic view of three steps involved in binding a single or a chain o**f** Ubiquitin. Figure copied from Nandi et al. 2006 (4).

2 Aims

The project has two aims:

1. To characterize which domains of MITF are involved in nuclear localization.

2. To determine which regions of MITF are involved in determining stability of MITF.

To achieve the aims of the study we aimed to answer the following questions by producing mutated versions of MITF-M in an EGFP reporter vector and then determine effects on nuclear localization and protein stability. The specific research questions asked are:

1. Which domains of the MITF protein are involved in nuclear localization and can we identify a specific amino acid sequence that represents a nuclear localization signal (NLS)?
2. Which protein domains of MITF affect protein stability and degradation and can we identify specific amino acids that are important for stability and degradation?
3. Through which protein degradation pathway is MITF degraded? Are there perhaps multiple pathways at work?

3 Material and Methods

The melanocyte-specific M isoform of the mouse MITF cDNA was inserted into the multiple cloning site of the pEGFP-C1 (11) (Clontech) plasmid using HindIII and SacII sites to produce an open reading frame featuring both the N-terminal located EGFP and MITF. Mutations were made using the New England BioLabs Q5 Site directed Mutagenesis Kit and mutations confirmed by BigDye terminator v1.1 sequencing (Life technologies, California USA). Sequences were analysed using the BLAST and MAFFT multiple sequence algorithms, available through Benchling (www.benchling.com). All constructs were transfected into 501Mel and HEK 293T cells using the FuGene HD transfection reagent (Promega, Wisconsin, USA). Cells were cultured in DMEM (Dulbecco's modified Eagle medium) with glutamax and 10% fetal bovine serum at 37C in 5% CO2 and then seeded on 8-well slides or a 6 well plate, cultured overnight and then incubated for 24 hour before fixing for imaging or for harvesting for westerns.

3.1 The EGFP-MITF fusion protein

The MITF-M (isoform2) had been inserted into a pEGFP-C1 plasmid previously (11). This construct (figure 1.) was the starting point and was the template used to produce all the mutated forms of MITF discussed in this project. Using an EGFP plasmid allowed us to forego antibody stainings and generate an efficient protocol to fix and stain samples in a short time thus allowing the study of many different constructs. In addition, using a GFP tag allows the analysis of mutated forms of MITF in melanoma cells that express endogenous MITF.

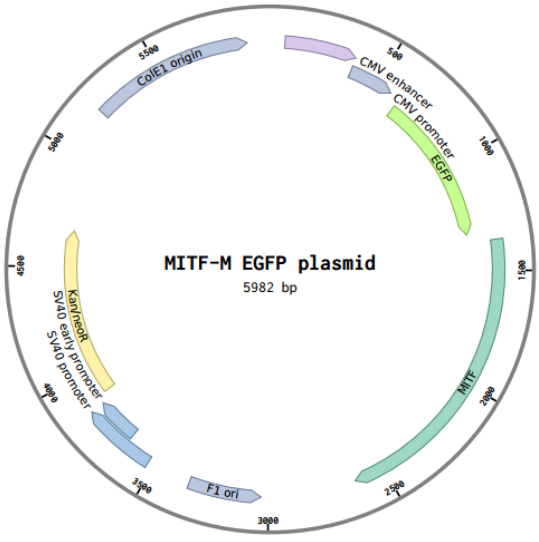

Figure 5. MITF-M insert in the pEGFP-C1 plasmid. The plasmid has a kanamycin antibiotic resistance cassette.

3.2 Transient transfection protocol for confocal imaging

When transiently transfecting cells, we seeded them to the density of $3x10^4$ cells in 250 µl of media in an 8 chamber slide for confocal imaging and $3x10^5$ cells in 3 ml in 6 well plate for western blot analysis. Cells were cultured overnight before transfection. To prepare the DNA complex for transfections we prepared a solution containing 0.25 µg of DNA in DMEM without FBS in a total volume of 25 µl. Then we added 0.7 µl of the fugene transfection reagent. The DNA complex solution was incubated for 5-10 minutes and then added to the wells to be transfected. Cells were then incubated for 24 hours at 37°C with 5% CO_2 in an incubator before treatment or harvesting.

3.3 Formaldehyde fixation and counterstaining of confocal samples

For imaging GFP transfected cells, the cells were fixed with formaldehyde. We added 250 µl of 4% formaldehyde (without methanol) to the media in each well and incubated for 2 minutes. Next all liquid was removed from the cell chambers and 4% formaldehyde added and incubated for 15 minutes. The cells were then washed once with PBS. Next the cells were permeabilized with 0.1% triton X-100 in PBS for 8 minutes. The cells were then washed three times for 5 minutes each time with PBS. Nuclear stain was added and the solution incubated for either 5 (when staining for DAPI) or 15 (when staining with TOPRO3) minutes. The samples were washed once in PBS for 5 minutes. All liquid was then removed off the samples, the plastic chamber removed, and the slides mounted with Fluoroshield and then covered with a coverslip.

3.4 Formaldehyde fixation and immunostaining of confocal samples

For imaging antibody stained cells, we added 250 µl of 4% formaldehyde (without methanol) to the media in each well and incubated for 2 minutes. The 2% formaldehyde-media mixture was then removed and 4% formaldehyde added and incubate for 15 minutes. The samples were then washed once with PBS and then permeabilized with 0.1% trition X-100 in PBS for 8 minutes. The samples were then washed with PBS 3 times, 5 minutes each step. The samples were then blocked for one hour at room temperature with blocking buffer (0.25% BSA, 0.05% trition X-100, and 5% goat serum in PBS). The samples were then stained with primary antibody (1D2 MITF or C5 MITF) in PBS containing 0, 25% BSA overnight at 4°C.

The samples were then washed 3 times with PBT (0.25% BSA, 0.05% trition X-100 in PBS) and then incubated with secondary florescent antibodies diluted in PBT for 1 hour at room temperature. The samples were then washed two times with PBT and once with PBS, 5 minutes each step. Nuclear stain was then added and incubated for 5 minutes with DAPI or 15 minutes with TOPRO3. The samples were then washed once in PBS for 5 minutes and all liquid removed off the samples, the plastic chamber removed, and the slides mounted with Fluoroshield and covered with a coverslip.

3.5 Methanol fixation and immunostaining for confocal imaging

Media was aspirated off the chamber slides and cells covered to a depth of 2-3 mm with ice cold methanol. The cells were fixed for 15 minutes at -20 °C. The fixative was aspirated and the wells rinsed three times with PBS for 5 minutes each time. Samples were blocked in blocking buffer (1X PBS/5% NGS 0.3% triton X-100) for 1 hour at RT and then stained with primary antibody (LC3,GFP;SILV,LAMP2) in antibody buffer (1X PBS / 1% BSA / 0.3% triton X-100) overnight at 4°C. The cells were then washed 3 times for 5 minutes with PBS and then stained with fluorescent secondary antibodies diluted in antibody buffer for 1 hour at room temperature. The samples were stained with DAPI for 5 minutes, then washed once in PBS for 5 minutes, all liquid removed off the samples, the plastic chamber removed, and the slides mounted with Fluoroshield and coverslip. The protocol used for antibody staining can be found in more detail online at: http://www.cellsignal.com/common/content/content.jsp?id=if-methanol-fixation.

3.6 Quantification of total protein using western blot.

First the media was removed from the cells and the cells washed once with cold PBS buffer. The samples were then incubated for 10 minutes in 100 µl of RIPA buffer (1/1000 PMFS, 1/100 protease inhibitor cocktail.). The cells were then scraped from the wells and the sample sonicated for 5 minutes using a water bath sonicator. Samples were then spun down for 15 minutes at 16,000g at 4°C. Then 80 µl of supernatant were mixed in sample buffer. The samples were then boiled for 5 minutes at 96°C and size separated using SDS gel electrophoresis (5% UTB 8% LTB), first for 20 minutes at 85 volts and 400 amps, then for 1 hour at 120 volts and 400 amps. Samples were then transferred to membrane, for 1.5 hour at 90 volts and 400 amps. The membrane was then blocked for 1 hour at room temperature. The membrane was then incubated with primary antibodies (GFP, β actin, P62) overnight, washed with TBS and then incubated for 1 hour with secondary antibodies. The membrane was then washed again and imaged using an Odyssey scanner.

3.7 Confocal microscopy

Confocal images were taken on Zeiss 510 Pascal and Olympus FLV1200 confocal microscopes. All images of constructs were taken using 40X magnification. Intensity levels were adjusted to the highest setting without causing overexposure; no background was filtered out. This was done so the localization of different quantities of the MITF-EGFP fusion protein could be seen in one image. Co-location images were taken with 60X magnification and images of cells treated with inhibitors were also taken at 60X magnification using the untreated wild-type cells as an intensity set point for all images.

3.8 Cell treatments

To define the protein degradation pathways involved in MITF degradation we treated transiently transfected cells for 2 hours with the inhibitors, cyclohexamide to stop protein expression, and then cyclohexamide in combination with either MG132 (a proteasome inhibitor) or chloroquine (CQ, an inhibitor of lysosomes. The idea was to see if we could get a clearer picture of MITF degradation by inhibiting protein expression and determining effects of MG132 and CQ.

Table 1. Inhibitors used in degradation assay. Inhibitors used, their concentration and function.

Chemical	Concentration	Function
Cyclohexamide	20 µg/ml	**Protein synthesis inhibitor**
MG132	10 µg/ml	**proteasome inhibitor**
Chloroquine	10 µg/ml	**Autophagy inhibitor**

4 Results

4.1 Overexpressed MITF, EGFP tagged MITF and endogenous MITF are all located in the nucleus

In order to investigate the subcellular localization of MITF, we fused the melanocyte-specific M-isoform of MITF to the carboxyl-end of green fluorescent protein (EGFP). To determine if this fusion protein accurately represents the subcellular localization of MITF, we compared transiently transfected cells to untransfected cells stained for endogenous MITF. We used two cell lines for our analysis; human embryonic kidney cells (HEK 293T) and human melanoma cells (501Mel). While the 501Mel melanoma cells express high levels of endogenous MITF, the HEK 293T cells do not express endogenous MITF. We included HEK 293T cells in our analysis to have the possibility of eliminating any effect that endogenous MITF might have on different mutant overexpressed forms of the protein (Figure 6). We stained untransfected 501Mel cells with an anti-MITF antibody (MITF-C5 antibody) and observed nuclear localization of the endogenous MITF with a small portion present in the cytoplasm (Figure 6).

The same pattern was also observed both when we transfected HEK 293T cells with an untagged MITF construct and stained for MITF (figure 6). We also saw the same pattern when we transfected either HEK 293T or 501Mel cells with the EGFP-MITF fusion construct (figure 6). These results indicate that overexpression of an untagged MITF or the EGPF-MITF fusion had no discernible effect on MITF nuclear localization and we were able to use transiently transfected overexpressed EGFP-MITF.

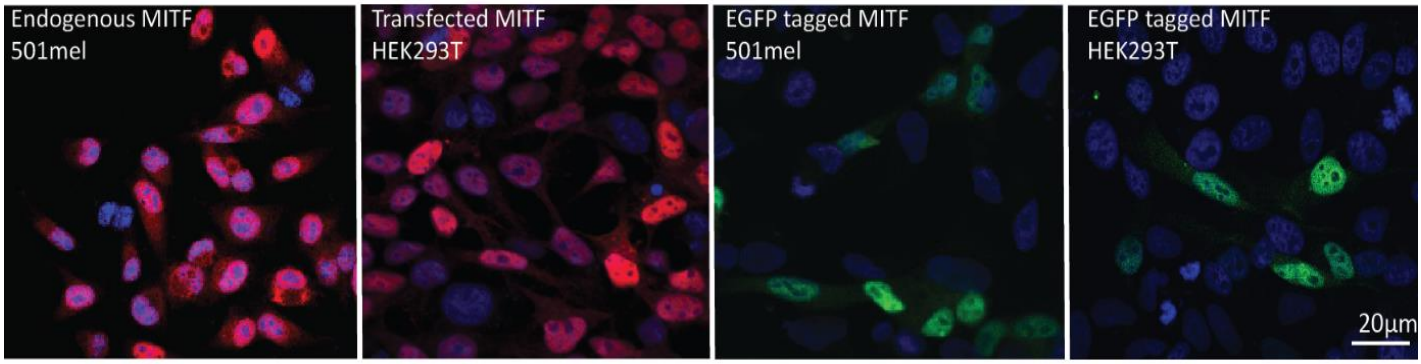

Figure 6. The MITF and GFP-MITF proteins are located in the nucleus. A. Antibody staining of endogenous MITF protein in 501Mel cells. B. Antibody staining of transfected MITF in HEK 293T cells. MITF-EGFP fusion protein in 501Mel cells. C. MITF-EGFP fusion protein expression.

4.2 MITF calculated size

For analysing the effect different parts of MITF on the subcellular localization of the protein, we generated a number of truncated EGFP tagged MITF mutants. We started by making sure that these truncated tagged MITF proteins would be actively imported into the nucleus based on size. It has been shown that proteins larger than 40 kDa are actively imported but ones smaller diffuse into the nucleus. Using a.a. calculator available online (http://www.bioinformatics.org/sms/index.html) we calculated the size of our EGFP tag, MITF and its truncated counterparts. All our constructs are larger than 40 kDa and should thus not diffuse into the nucleus but require Importin mediated transport across the nuclear envelope.

Table 2. Size calculation of constructs. Calculation of both MITF and EGFP as well as the total protein size.

MITF-Constructs	Approx. Size kDa	EGFP size kDa	Total size kDa
Wild-type	46,8	26,8	73,6
258x	29,1	26,8	55,9
278x	31,6	26,8	58,4
298x	33,9	26,8	60,7
316x	35,7	26,8	62,5
del1-70	38,9	26,8	65,7
del1-120	33,3	26,8	60,1
del1-170	27,9	26,8	54,7
del1-220	22,1	26,8	48,9

4.3 MITF truncation does not affect nuclear localization

In order to determine which domains of MITF are involved in nuclear localization of the protein, we produced truncated forms of MITF lacking portions of the N- and C-termini of MITF. The N-terminal truncations where made by deleting residues 1-70, 1-120, 1-170 and 1-220 of MITF from the EGFP-MITF fusion construct, starting from the last residue of GFP's (Table 1). C terminal truncations were made by inserting a stop codon at the indicated positions, resulting in protein truncations. In addition to the truncated forms of MITF we also produced site specific mutations based on the literature. One of these mutations that did not produce a change from the Wt. phenotype but is worth mentioning is when we mutated 3 of the 4 leucinines causing dimerization of the leucine zipper to phenyl alanine (L267/274/281). This mutated construct is still located in the nucleus (not shown).

Table 3. MITF truncations produced. List of truncation produced and a short description of the mutation.

N-terminus	Mutation	C-terminus	Mutation
Del1-70	First 70 a.a. deleted	**258X**	Stop codon inserted at a.a. 258
Del1-120	First 120 a.a. deleted	**278X**	Stop codon inserted at a.a. 278
Del1-170	First 170 a.a. deleted	**298X**	Stop codon inserted at a.a. 298
Del1-220	First 220 a.a. deleted	**316X**	Stop codon inserted at a.a. 316

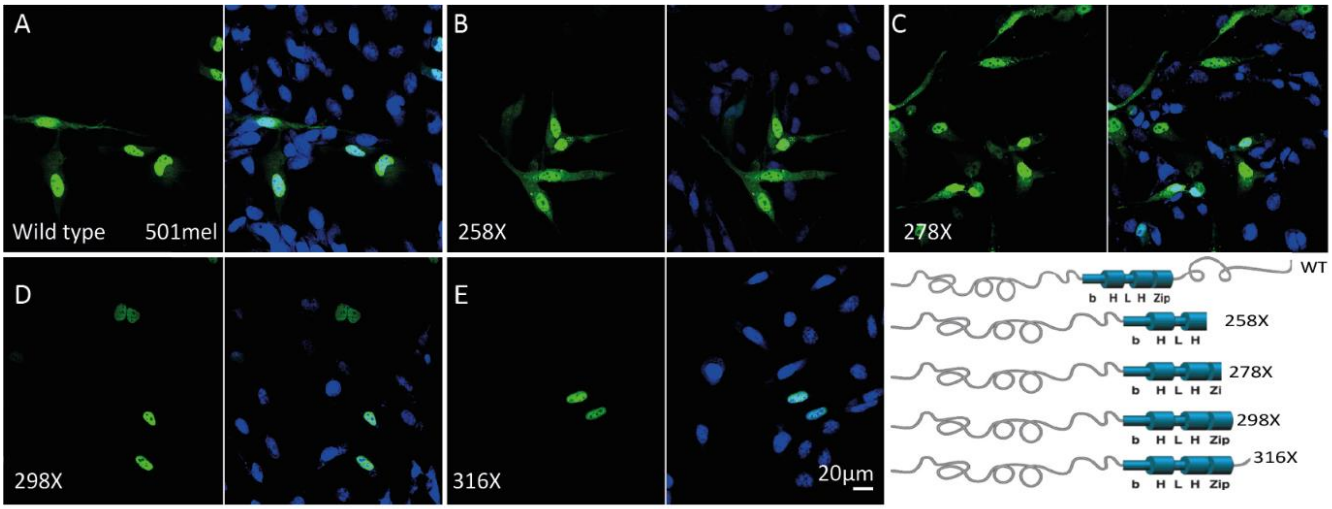

Figure 7. Subcellular localization of MITF C-terminal truncations. A. Wild-type EGFP-MITF fusion protein transfected in 501Mel melanoma cells. B-E. EGFP-MITF fusion proteins truncated at residue 258, 278, 298 and 316 transfected in 501Mel cells.

Cells transfected with the wild-type EGFP-MITF fusion protein have the protein mainly located in the nucleus with a small portion of the protein in the cytoplasm (figure 7A). The truncations 258X and 278X show the same phenotype (figure 7B, C). However, the 298X and 316X truncations are exclusively located in the nucleus and no protein can be detected in the cytoplasm (figure 7 D, E).

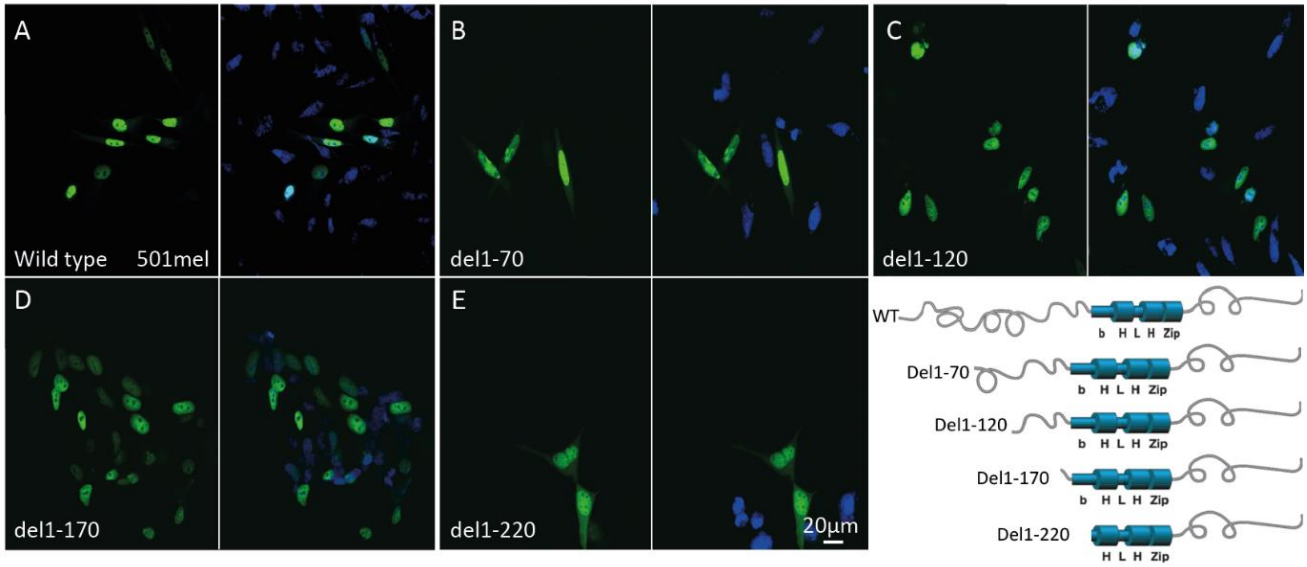

Figure 8. Subcellular localization of MITF N-terminal truncations. A. Wild-type EGFP-MITF fusion protein transfected in 501Mel melanoma cells. B-E. EGFP-MITF fusion proteins truncated between a.a. 1-70, 1-120, 1-170 and 1-220 transfected in 501Mel cells.

Transfecting the N-terminal truncations into 501Mel cells revealed that del1-70 behaved like the wild-type protein, with predominant nuclear presence but some component in the cytoplasm (figure 8 A). The del1-120 truncation was also in both compartments but with less presence in the cytoplasm. The del1-170 mutant fusion protein was exclusively nuclear (figure 8 D) producing the same phenotype as 298X and 316X. Interestingly del1-220 which lacks the basic domain of MITF was similar to Wt. (f 8 E). To summarize, none of the truncations analysed had major effects on nuclear localization although some resulted in reduced presence in the cytoplasm.

4.4 The DNA binding domain of MITF is required for nuclear localization

The basic DNA binding domain of MITF is a short motif of basic amino acids which contain a stretch of 4 arginines which resemble a monopartite NLS. The DNA binding domain has previously been suggested to contain a NLS (28). In order to determine if these four arginines represent a bona-fide nuclear localization signal, we generated multiple different constructs where these arginines were mutated to alanine in different pairs (AARR, RRAA, ARRA, RAAR), or all four simultaneously. Mutating pairs of 2 arginines simultaneously resulted in less GFP-MITF protein in the nucleus and more in the cytoplasm than observed with the Wt. GFP-MITF construct (figure. 9 A, C-F). However, mutating all 4 arginines to alanine resulted in exclusive presence in the cytoplasm (figure 9 B), a subcellular location that is distinctly different from the wild-type construct (figure 9 A).

Deletion of one of the four arginines, del217, discovered in the $MITF^{mi}$ mouse mutation as well as in humans with the pigmentation and deafness disorder Waardenburg Syndrome Type 2A, has been suggested to affect nuclear localization of the protein (ref). It also affects DNA binding leading to a protein that cannot bind DNA (1). When this mutation was generated in an M-MITF construct, without a fusion to GFP, the resulting protein was primarily located in the nucleus, with a small cytoplasmic component, similar to wild-type (figure 9) (12). This suggests that the four arginines in the basic

domain represent a classical nuclear localization signal and that they are all important for this function. Since the del217 mutation cannot bind DNA it is unlikely that nuclear retention of MITF depends on DNA binding ability.

Interestingly, the deletion construct del1-220 was located in the nucleus, despite lacking the 4 arginines in the basic domain. This suggests that other domains, located after residue 220, are also important for nuclear localization. There are plans to produce new constructs to resolve this issue such as producing a del1-220 mutation without a tag to verify the effects of this mutation and that it does not depend on the GFP protein.

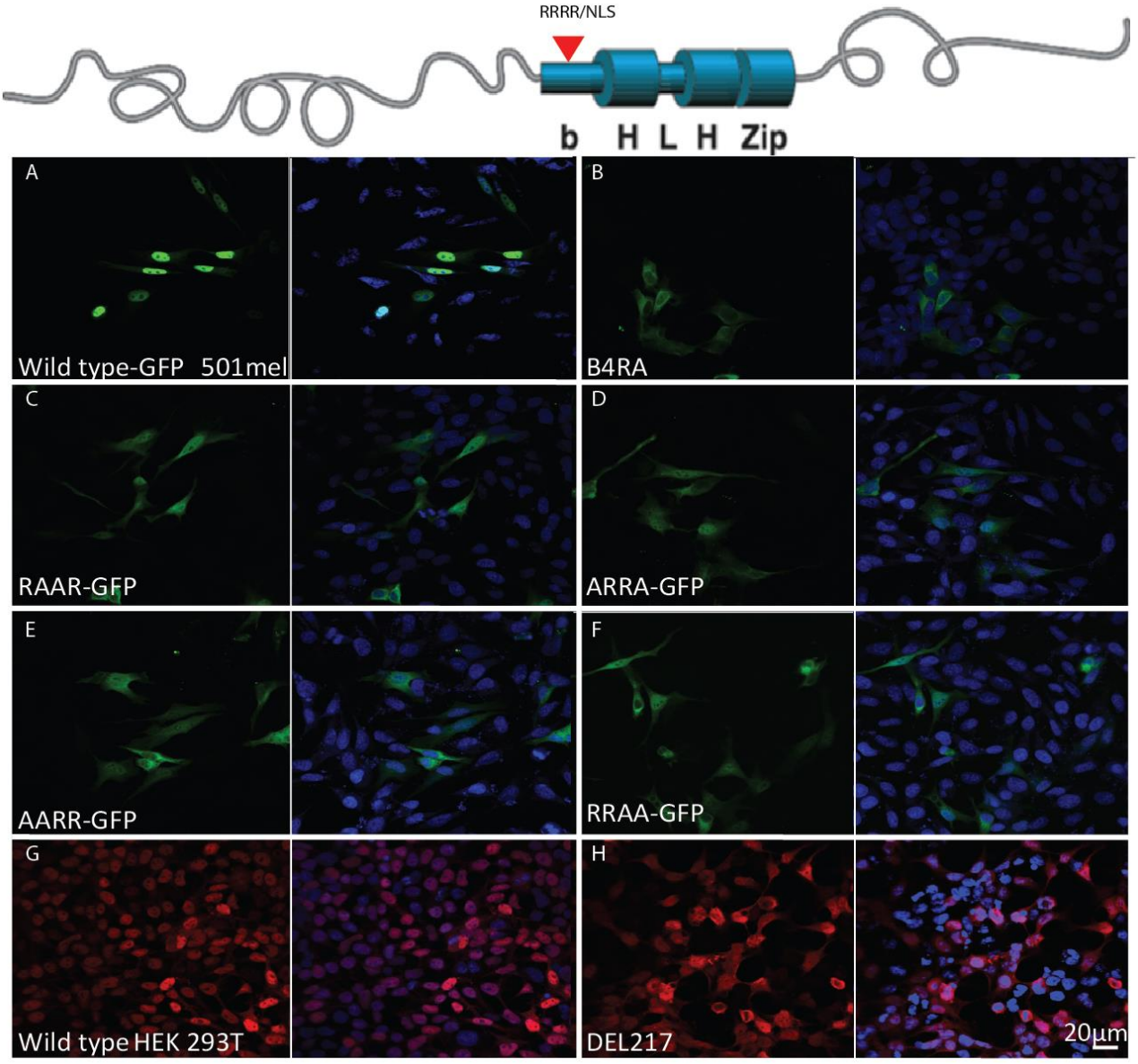

Figure 9. Effects of the basic domain on subcellular location of MITF: A Wt. EGFP-MITF construct transfected into 501Mel melanoma cells. B-F. EGFP-MITF fusions with the indicated mutations in the 4 arginines in the DNA binding domain in 501Mel melanoma cells. G. HEK 293T cell transfected with wild-type MITF-M and stained with MITF primary and Cy3 secondary antibody. H. HEK 293T cell transfected with MITFmi (del217) and stained with MITF primary and Cy3 secondary antibody.

4.5 MITF double mutant

Although the truncations above did not affect nuclear localization we did observe that the constructs del170 (figure. 8 D), 298X and 316X (figure. 7 D, E) resulted in exclusively nuclear GFP-MITF fusion proteins. Since residue 316 is part of a SUMOylation site that has been found to be mutated in melanoma families (E318K - refs), we decided to investigate this further. Thus, we combined the 316X mutation (fully nuclear, figure. 10 C) with the B4RA mutation (exclusively cytoplasmic, figure 10 B.). The double mutant protein resulted in a cytoplasmic punctate pattern (figure. 10 D), suggesting location to cytoplasmic vesicles or organelles.

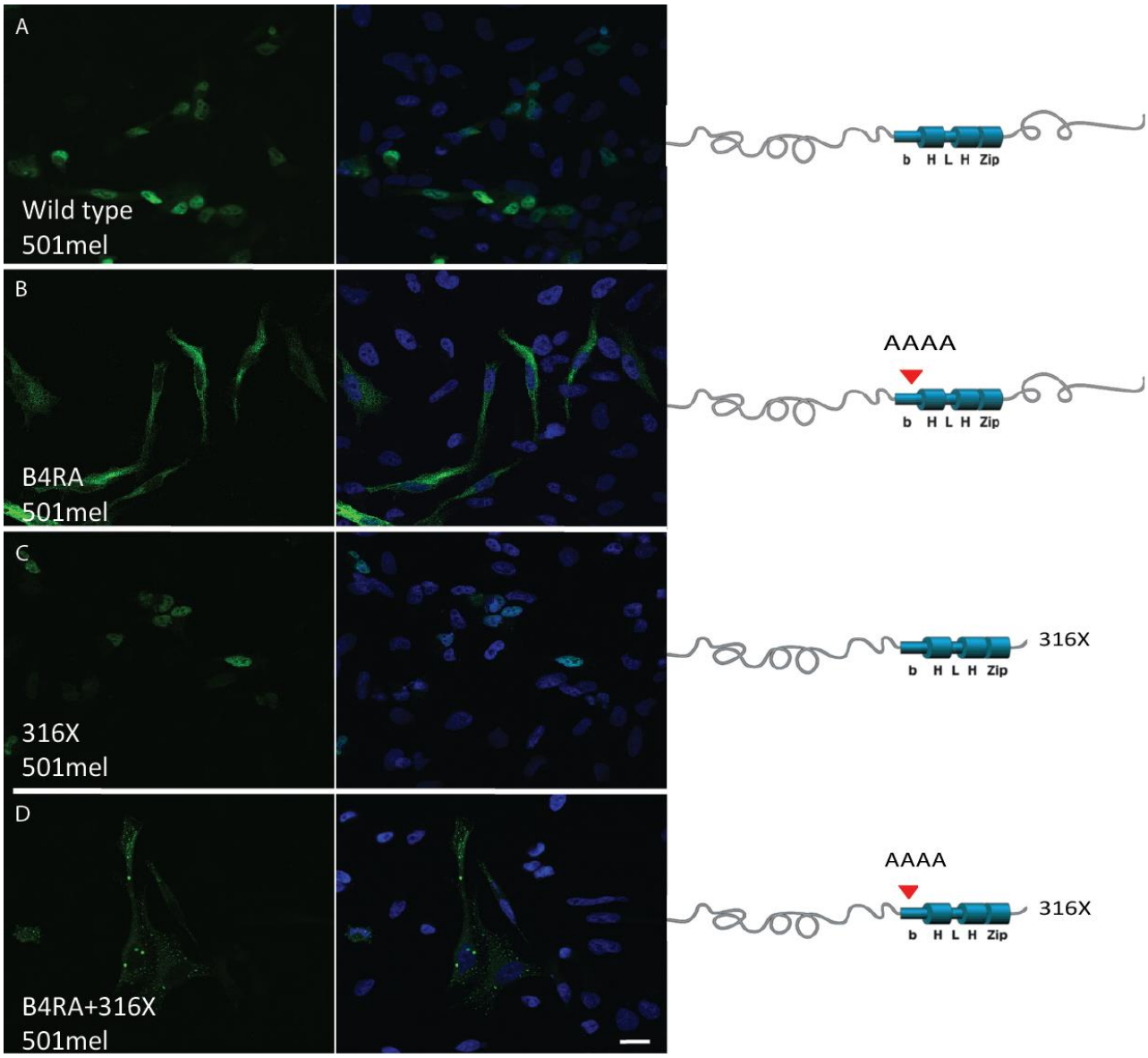

Figure 10. Effects of double mutations. A. Wild-type EGFP-MITF fusion proteins transfected into 501Mel cells. B. EGFP-MITF fusion protein with a.a. 214-217 mutated to alanine in 501Mel cells. C. EGFP-MITF fusion protein truncated at a.a. 316X in 501Mel cells. D. EGFP-MITF fusion protein carrying 2 mutations simultaneously, a.a. 214-217 mutated to alanine and a truncation at a.a. 316 in 501Mel cells.

To determine if the double mutant GFP-MITF protein was present in specific vesicles, we stained the cells for the melanoma marker SILV (PMEL), the lysosomal and autolysosomal marker LAMP2 (CD107b**)** and for the autophagosomal and autolysosomal marker LC3 (MAP1LC3A) and also visualized the GFP protein. The results showed no co-staining of the B4RA; 316X double mutant GFP-MITF protein with either SILV or LAMP2. However, this construct co-localized with LC3, suggesting that this mutant construct is present in or on the autophagosomes or auto-lysosomes (figure. 11). In order to determine if the familial melanoma mutation $MITF^{E318K}$ was also involved in associations with the autophagosomes, we generated a double mutant construct simultaneously carrying the B4RA and E318K mutations. On its own, the $MITF^{E318K}$ does not affect localization; the mutant protein is nuclear (figure. 12). However the B4RA; E318K double mutant was cytoplasmic similar to the B4RA mutation alone, and did not exhibit punctate staining (figure 12). Thus, the SUMOylation site does not seem to result in the MITF protein locating to the autophagosomes.

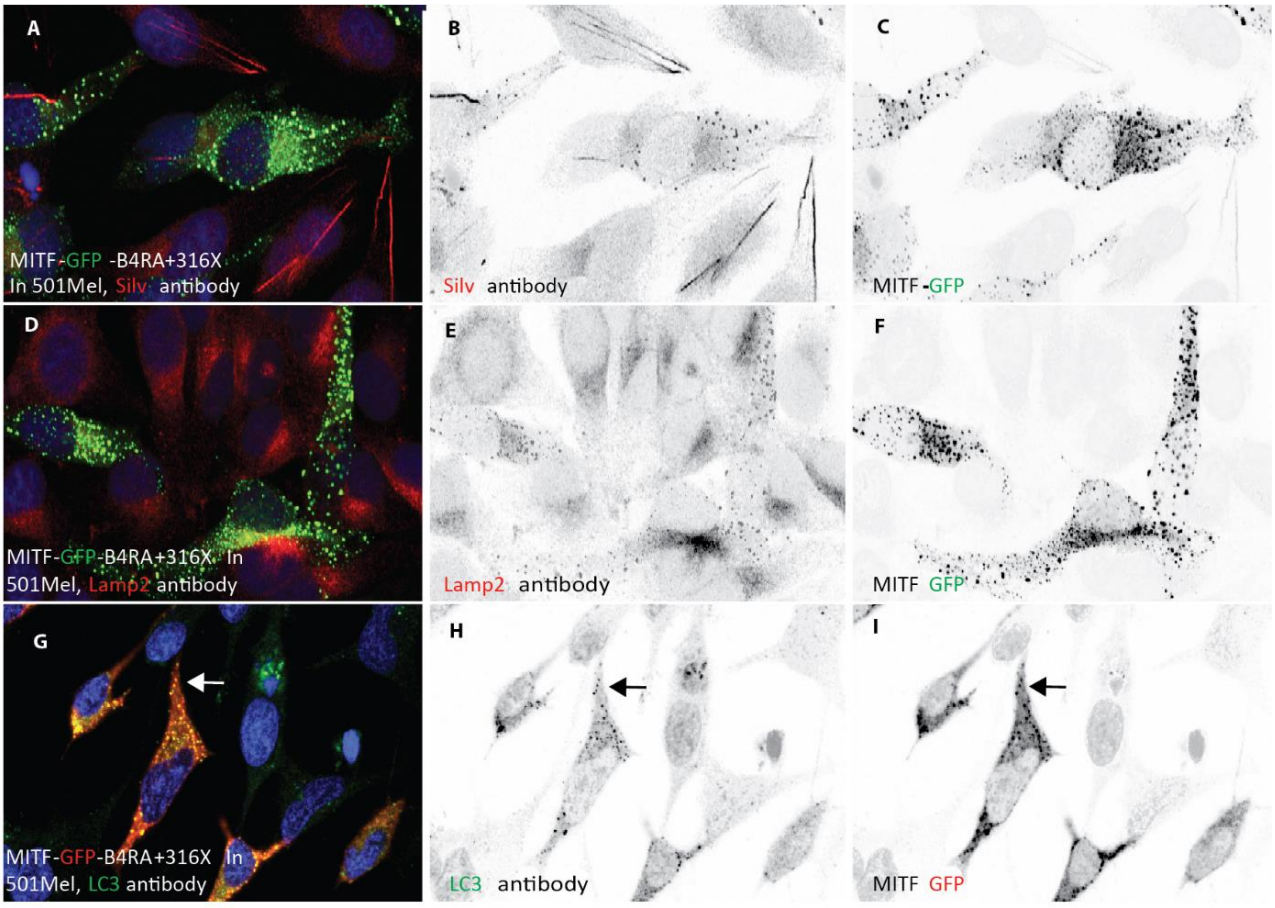

Figure 11. Co-localization of truncated MITF protein with autophagosomes. A. 501Mel cells transfected with the indicated EGFP-MITF fusion proteins and stained with SILV primary and Cy3 secondary antibodies. B, C. a single channel of image A showing negative grayscale image. D. 501Mel cells transfected with EGFP–MITF fusion protein and stained with Lamp2 primary and Cy3 secondary antibodies. E, F. A single channel of image D showing negative grayscale image. G. 501Mel cells transfected with EGFP-MITF fusion protein and co stained with anti LC3 and anti GFP primary and Cy3 and Alexa488 secondary antibodies. H, I a single channel of image G showing negative grayscale. The arrow points to dots common to both LC3 and GFP signals.

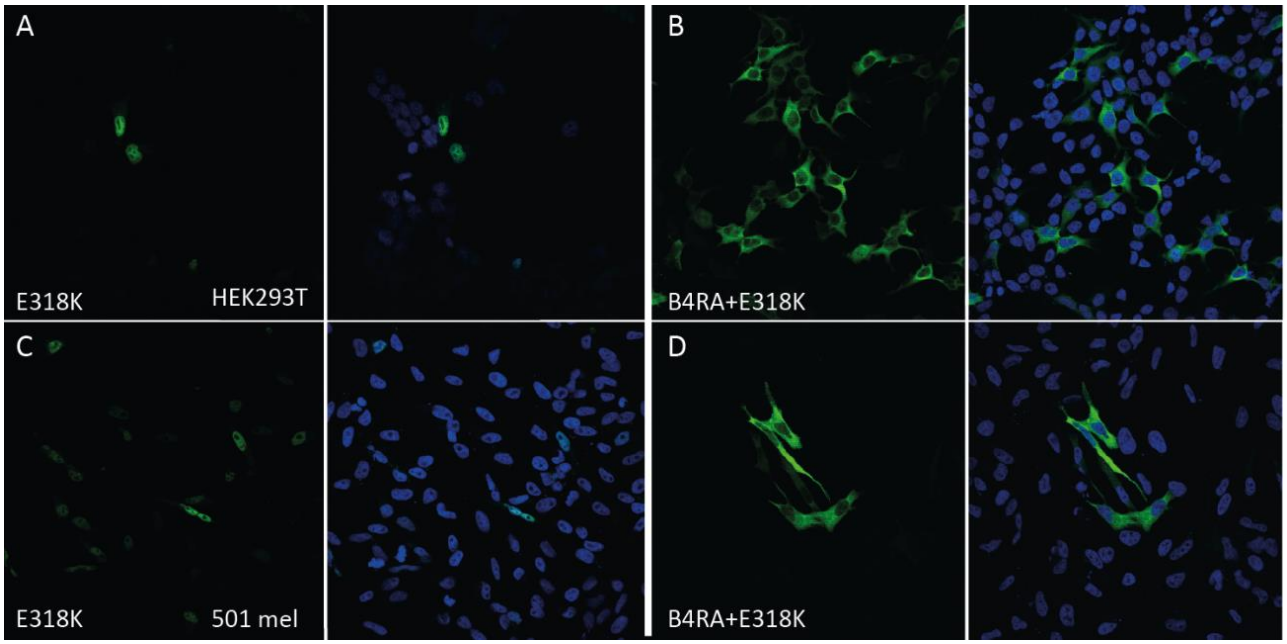

Figure 12. The E318K mutation does not replicate the 316X truncation phenotype. A, C E318K EGFP-MITF B, D B4RA+E318K double mutation all transiently transfected into 501Mel and HEK 293T cells.

4.6 MITF protein stability

The C-terminus of MITF has been implicated in protein degradation. In order to characterize if degradation is involved in the exclusive nuclear presence of 298X and 316X and to determine if the double mutation (B4RA+316X) was being degraded through specific degradation pathways, we used cyclohexamide (CHX) to stop protein synthesis and also used the proteasome inhibitor MG132 and the lysosomal inhibitor CQ and determined effects on protein location and turnover.

To determine the difference in protein turnover, we transfected 501Mel cells with wild-type and mutant GFP-MITF constructs, incubated the cells for 22 hours and then treated them for 2 hours with inhibitors. We imaged the transfected cells with and without treatment.

Treatment of the wild-type GFP-MITF protein with CHX lead to a reduction of intensity as judged by confocal microscopy (figure. 13A, B). However, when treated with CHX and MG132 or CHX and CQ in combination, we observed less reduction in protein intensity (figure. 13 C, D). When the B4RA construct was treated with CHX an increase in GFP intensity was observed, suggesting increased stability of the cytoplasmic protein (figure. 13 E, F). This increased intensity was not observed in the presence of the MG132 and CQ inhibitors (figure. 13 G, H).

Interestingly both the 316X and B4RA+316X mutant proteins showed a reduction in the GFP signal when treated with CHX (Figure 8I, J, M, and N). In particular, the vesicles observed in the double mutant were absent (figure. 13N). In the presence of the CQ and MG132 inhibitors these two mutations are present at increased intensity again (figure 13 K, L, O, and P). Importantly, the dot-like staining of the double mutant comes back, particularly when treated with CQ. This suggests that degradation is involved in regulating MITF concentration in the cytoplasm, that the C-terminus is likely

to contain a degradation signal and that the lysosomal pathway is important for regulating MITF stability, in addition to the proteasomes. To exclude the bias above we turned to western blots to analyse the difference in relative protein concentration.

Since cells were not synchronized with respect to cell cycle, there is considerable heterogeneity in the phenotype of the cells. This might result in a selection bias in terms of which cells were imaged. However, we believe that the experiment indicated that the cyclohexamide-treated cells actually showed a higher GFP intensity overall. We also observed that images of the 316X truncation and the double mutant showed recovery of cytoplasmic MITF when treated with CHX and CQ (figure 13 L,P) . The double mutant also showed a partial recovery when treated with CHX and MG132 (figure 13 O).

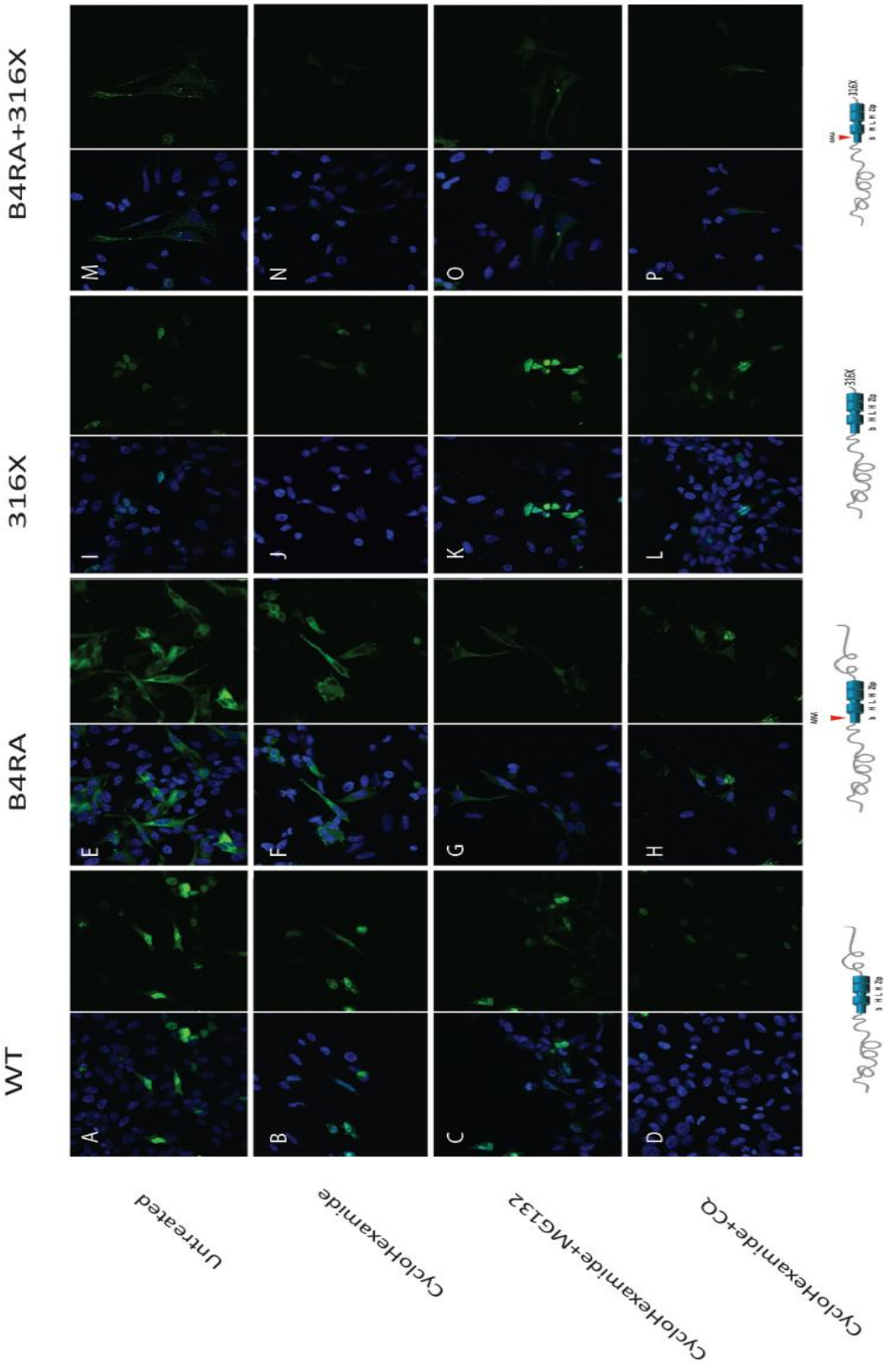

Figure 13. Effects of mutations on protein turnover. Wt. and mutated constructs of EGFP-MITF treated with inhibitors to analyse the effects of mutations on protein degradation. 501Mel cells transiently transfected with EGFP-MITF and treated for 2 hours.

To exclude the possible bias discussed above we turned to western blots to analyse the difference in relative quantities of MITF-EGFP proteins in cells transfected with wild-type GFP-MITF and B4RA+316X mutant constructs. We repeated the inhibitor experiment and harvested the cells for western blot analysis and compared the relative MITF quantities of wild-type GFP-MITF and B4RA+316X mutant proteins, with or without treatment with CHX, CHX and MG132 or CHX and CQ. Treatment of cells transfected with the wild-type GFP-MITF protein with CHX leads to reduced concentration of the wild-type MITF protein, suggesting that the protein is being degraded. Treatment with MG132 does not affect this degradation process whereas treatment with CQ clearly inhibits the degradation of MITF. This suggests that MITF is degraded through lysosomal degradation processes. Treatment of cells transfected with the B4RA+316X double mutant GFP-MITF protein with CHX does not affect stability of the fusion protein. This suggest that the protein may be missing a domain involved in regulating MITF degradation in the cytoplasm. Similarly, treatment with MG132 does not affect stability whereas no protein was observed when the cells were treated with CQ in addition to CHX. This experiment needs to be repeated before we can draw definite conclusions from it but it seems that MITF is primarily degraded through a lysosomal degradation pathway and that the C-terminus of MITF contains a domain involved in regulating stability.

The western blot was also stained with antibodies against p62, an autolysosomal marker. A difference in p62 intensity was seen when the cells transfected with wild-type GFP-MITF protein were treated with CQ in addition to CHX, but not when they were treated with CHX alone or with CHX and MG132. However, p62 staining was reduced in all treatment groups for the B4RA+316X double mutant GFP-MITF proteins. At this point, we are not sure what this means and are working on repeating this entire experiment.

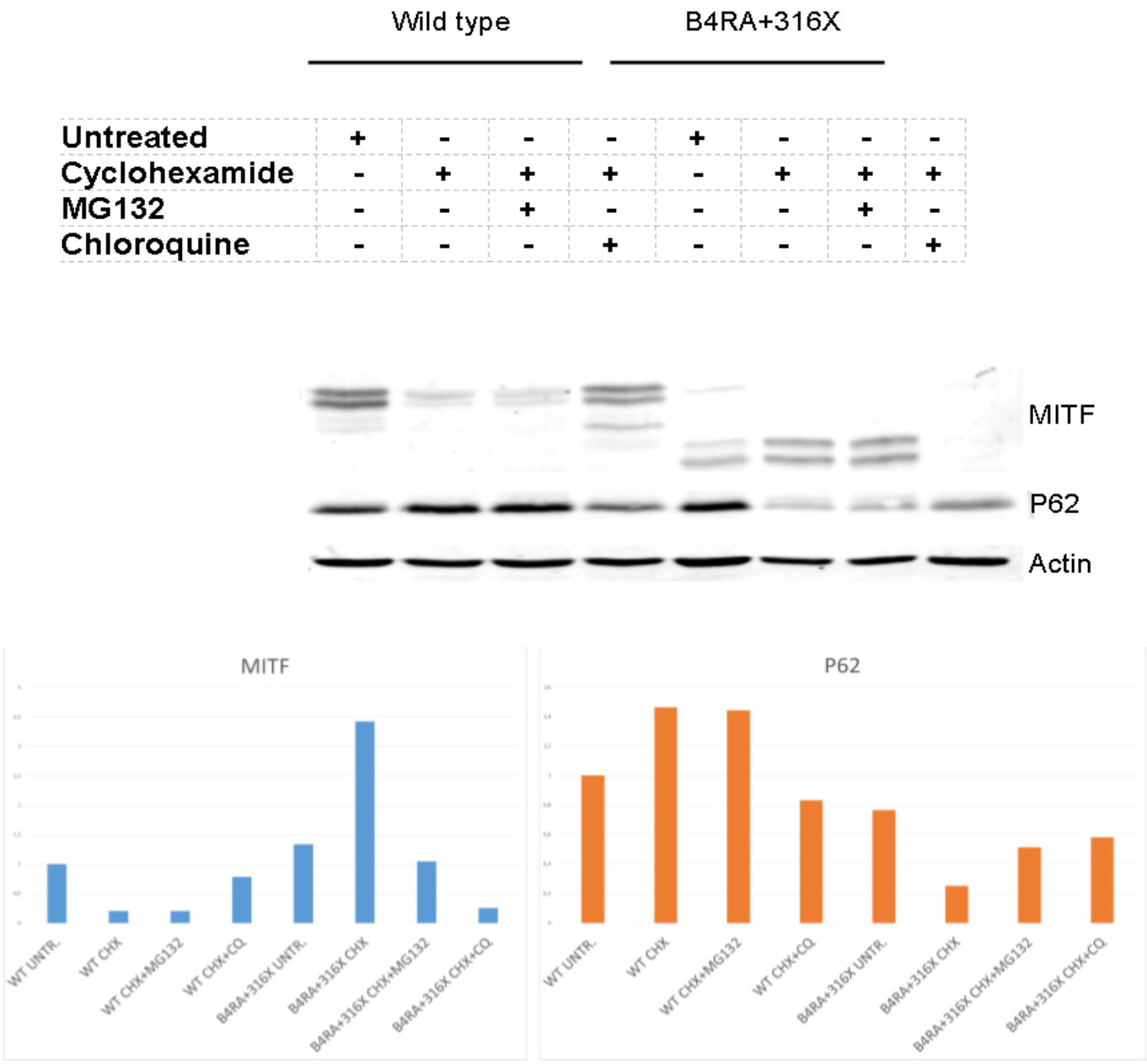

Figure 14. Quantitative Western blot of Wt. and mutated MITF with and without inhibitors.
501Mel cells where transfected with Wt. and B4RA+316X mutation of EGFP-MITF.

5 Discussions

5.1 Nuclear localization

A monopartite NLS that binds to one of the Importin-α subtypes is a short motif of positively charged lysines or arginines (17). The mutations we produced where we mutated the four arginines of the DNA binding domain in the basic domain to alanine (B4RA), resulted in exclusive presence of the protein in the cytoplasm showing that the DNA binding domain of MITF is crucial to nuclear localization and acts as a nuclear localization signal. For further analysis we produced constructs where 2 of the 4 arginines where mutated to alanine. These constructs resulted in proteins that were both nuclear and cytoplasmic, but with more protein in the cytoplasm. This further suggests that MITF's DNA binding domain also serves as a nuclear localization signal.

We believe that the results presented in this thesis support the hypothesis that MITF is imported into the nucleus by the classical nuclear localization transport mechanism.

In light of the B4RA mutation, it is interesting that del220 is still nuclear. This result might signify one of two things. First it could be caused by an artificial NLS produced where GFP and MITF meet, second it might be caused by a second NLS either a classical or non-classical NLS located elsewhere in the protein. Thus, current work is aimed finding a possible alternate nuclear localization signal.

If future work were to continue on nuclear localization of MITF, it would be very interesting to use the EGFP tagged constructs made in this project and perform a co– immunoprecipitation experiment. A Co-IP could enable us to pull down the Importins bound to MITF and identify them on a western blot. Confirming which Importins bind MITF could lead to further questions than just to identify the pathway. It was recently presented that Importin α2 could bind to the transcription factors Oct6 and Brn2 (N-Oct-3), thus forming a transport incompetent complex. During neural differentiation in mouse embryonic stem cells, expression of Importin α subtypes is switched from α2 to α1, enabling import of Oct6 and Brn2. Brn2 also regulates melanoma proliferation and is upregulated by BRAF. Brn2 represses MITF expression to the point that two distinct subpopulations can be identified in melanomas: one Brn2 positive the other MITF positive (29) and in the light of this inverse expression the import dynamics of these two transcription factors could lead to novel insight into melanocyte development as well as skin cancer.

5.2 MITF protein stability and degradation

Although the truncated forms of MITF we created were all located in the nucleus, some of the mutant proteins including Del1-170, 298X and 316X were exclusively nuclear. Due to the fact that 316X is a known mouse mutation (Steingrímsson et al. unpublished) and the fact that both this mutation and the E318K mutation (found in melanoma families) affect a proposed SUMO-site in MITF, we decided to focus on the 316X mutation. A new publication indicates that 3 GSK3 phosphorylation sites (S397,S401, S405 with 409 as a priming site) increase MITF protein turnover by initiating poly Ubiquitination labelling of the protein for proteosomal degradation (30). When we put this mutation

together with the B4RA mutation, which resulted in the protein being exclusively cytoplasmic, the protein was now located in the autophagosomes. This might indicate that by placing all the protein in the cytoplasm, and by deleting the C-end of the protein, we have sensitized the system in order to detect which degradation pathways are involved in degrading MITF. Our results suggest that autophagosomes are involved in degrading MITF. An alternative hypothesis is that the effects we observe are simply due to the synthetic fusion protein we created and have nothing to do with the normal degradation of MITF. This needs to be tested by generating the same mutation without the GFP fusion. Autophagy is a catabolic process that degrades cytoplasmic proteins. In recent years models for selective autophagy have been revised and NRB1 and P62 that bind to ubiquitinated proteins and are also able to bind LC3 have been suggested as selection factors in selective autophagy (31). These selective autophagy models alongside research on ubiquitination have showed how different degradation pathways can not only make up for other blocked pathways but also have different roles in protein degradation and can even be specific to degradation of certain organelles (32).

The results from the inhibition experiments we performed are not consistent enough to draw definite conclusions at this time (Figure 9). Samples that are transiently transfected and treated with inhibitors such as CHX show a high phenotypic heterogeneity causing a bias in confocal imaging. This caused us to turn to Western blots and preliminary results are promising. Using CHX to inhibit protein synthesis is a common practice when looking at subcellular functions. It recently came to our attention that CHX has been suggested to inhibit autophagy through mTORC1 activation (33). Because of these findings we are continuing this experiment with and without CHX and we are also going to analyse the difference in MITF turnover between 501Mel cells and HEK 293T cells. However these results do indicate that Wt. MITF is degraded through the autophagy degradation pathway, a pathway that has not been linked to MITF before.

The C-terminal truncations resulted in MITF being exclusively located in the nucleus. As autophagy is specific to the cytoplasm it is possible that C-terminal truncations of MITF cause an increase in autophagic degradation. When we “overload” the cells cytoplasm with EGFP tagged truncation of MITF (B4RA+316X) we see a punctate pattern, and we know that mutations in the C-terminus decrease the proteasome degradation of MITF (30). Together these results suggest that if truncation of the C-termini causes a switch from a blocked pathway, the proteosomal pathway, to an active one, autophagy, as has been described before (32).

We also made B4RA+E318K a double mutation to see if we could produce the same phenotype by inhibiting the SUMOylation of a.a. 316. B4RA+E318K did not replicate the pattern of B4RA+316X (Figure 12). Our results are consistent with previous studies which show that SUMOylation does not affect protein stability or nuclear localization. Neither study was however done in melanoma cells (34, 35).

5.3 Next steps

Future work will build on the work described in this thesis. The results lead us to even more questions which we aim to answer in the near future. The first objective is to narrow the domain that is

responsible for the 316X phenotype down to a shorter a.a. sequence by removing parts of the C-terminus in 30 a.a. deletion sections, sequentially from a.a. 316 to the end of the protein at a.a. 419. We are also going to analyse further the N-terminus by producing N-terminal truncations bigger than del1-220 such as del1-258 and del1-278. These will help us assess if other parts of MITF than the DNA binding domain are affecting nuclear localization of MITF. A recent paper reported novel GSK3 sites on the C-termini of MITF (30). We aim to make an EGFP tagged construct where we mutate these sites into alanine and visualize the effects in cells and compare the protein stability to Wt. on a western blot.

In addition to these clones we want to ligate both Wt. and the B4RA+316X mutations of MITF into phluorin expressing plasmid thus making a phluroin – MITF fusion protein. Phluroin is a mutated version of GFP that is pH sensitive such that pH change results in a color change (36). These pH sensitive MITF constructs would allow us to analyse the degradation of MITF in the vacuole pattern caused by B4RA+316X and see if the mutant is in fact inside acidic lysosomes or autolysosomes or if the protein is piling up in inside the cells.

Table 4. MITF constructs that will be produced, in this project. A list of construct to be produced along with the question they aim to answer.

MITF constructs to produce	**Research question**
MITF-EGFP + GSK3 (S397A, S401A, S405A)	Do the novel GSK sites from Plober.et al. affect subcellular localization?
MITF-EGFP + B4RA + GSK3 ->A (S397A, S401A, S405A)	Can we recreate the B4ra+316x mutation?
MITF-EGFP + B4RA + del1-170	Del1-170 is nuclear exclusive like B4RA+316X,
MITF-EGFP + Ndel-258	Further mapping off the roles of MITF‘s domain in subcellular localization and protein stability.
MITF-EGFP + Del-316-351	Which amino acids cause the nuclear exclusive phenotype of 316X?
MITF-EGFP + Del-352-386	Which amino acids cause the nuclear exclusive phenotype of 316X?
MITF-EGFP + Del-387-419	Which amino acids cause the nuclear exclusive phenotype of 316X?
MITF- Phluorin Wt. and B4RA+316X	PH sensing plasmid to detect vacuolar degradation of MITF
Differentially tagged MITF	Is EGFP affecting the truncated phenotypes?

6 Conclusions

We began this project to explain MITF's nuclear localization. In light of the interesting results of the truncated forms of MITF and the double mutant (B4RA+316X), we expanded our goals to include protein stability and answer the 3 following questions.

1. Which domains of the MITF protein are involved in Nuclear Localization and can we identify the NLS as a specific amino acid sequence?

   We show that the four arginines in the basic domain (a.a. 214-217) function as a nuclear localization signal.

2. Which protein domain of MITF affect protein stability and degradation and can we identify specific amino acids that are important for stability and degradation?

   We show that a part of the leucine zipper a.a. 278-298 is a region of interest that could explain autophagic degradation. These results indicate that there is more to degradation of MITF than has previously been reported.

3. Through which protein degradation pathway is MITF degraded or can there be multiple pathways at work?

   We show that MITF is not only degraded through the proteosomal pathway as has been previously established but also via autophagy.

References

1. Pogenberg V, Ogmundsdottir MH, Bergsteinsdottir K, Schepsky A, Phung B, Deineko V, et al. Restricted leucine zipper dimerization and specificity of DNA recognition of the melanocyte master regulator MITF. Genes & Development. 2012;26(23):2647-58.
2. Pumroy RA, Cingolani G. Diversification of importin-alpha isoforms in cellular trafficking and disease states. The Biochemical Journal. 2015;466(1):13-28.
3. Xie Y, Kang R, Sun X, Zhong M, Huang J, Klionsky DJ, et al. Posttranslational modification of autophagy-related proteins in macroautophagy. Autophagy. 2015;11(1):28-45.
4. Nandi D, Tahiliani P, Kumar A, Chandu D. The ubiquitin-proteasome system. Journal of Biosciences. 2006;31(1):137-55.
5. Arnheiter H. The discovery of the microphthalmia locus and its gene, Mitf. Pigment Cell Melanoma Reseach. 2010;23(6):729-35.
6. Steingrimsson E, Tessarollo L, Pathak B, Hou L, Arnheiter H, Copeland NG, et al. Mitf and Tfe3, two members of the Mitf-Tfe family of bHLH-Zip transcription factors, have important but functionally redundant roles in osteoclast development. Proceedings of the National Academy of Sciences of the United States of America. 2002;99(7):4477-82.
7. Shibahara S, Takeda K, Yasumoto K, Udono T, Watanabe K, Saito H, et al. Microphthalmia-associated transcription factor (MITF): multiplicity in structure, function, and regulation. The journal of investigative dermatology Symposium proceedings / the Society for Investigative Dermatology, Inc [and] European Society for Dermatological Research. 2001;6(1):99-104.
8. Levy C, Khaled M, Fisher DE. MITF: master regulator of melanocyte development and melanoma oncogene. Trends in Molecular Medicine. 2006;12(9):406-14.
9. Lu SY, Wan HC, Li M, Lin YL. Subcellular localization of Mitf in monocytic cells. Histochemistry and Cell biology. 2010;133(6):651-8.
10. Martina JA, Diab HI, Li H, Puertollano R. Novel roles for the MiTF/TFE family of transcription factors in organelle biogenesis, nutrient sensing, and energy homeostasis. Cellular and Molecular Life sciences : CMLS. 2014;71(13):2483-97.
11. Hansdóttir AG. Analysis of a suppressor mutation at the mouse Mitf locus. Háskólaprent: University of Iceland; 2004.
12. Grill C, Bergsteinsdottir K, Ogmundsdottir MH, Pogenberg V, Schepsky A, Wilmanns M, et al. MITF mutations associated with pigment deficiency syndromes and melanoma have different effects on protein function. Human Molecular Genetics. 2013;22(21):4357-67.
13. Berwick M, MacArthur J, Orlow I, Kanetsky P, Begg CB, Luo L, et al. MITF E318K's effect on melanoma risk independent of, but modified by, other risk factors. Pigment Cell Melanoma Research. 2014;27(3):485-8.
14. Van Allen EM, Wagle N, Sucker A, Treacy DJ, Johannessen CM, Goetz EM, et al. The genetic landscape of clinical resistance to RAF inhibition in metastatic melanoma. Cancer Discovery. 2014;4(1):94-109.
15. Kim DK, Morii E, Ogihara H, Lee YM, Jippo T, Adachi S, et al. Different effect of various mutant MITF encoded by mi, Mior, or Miwh allele on phenotype of murine mast cells. Blood. 1999;93(12):4179-86.
16. Motohiko Sato EM, Kimiko Takebayashi-Suzuki, Natsuo Yasui,, Takahiro Ochi YK, and Shintaro Nomura. Microphthalmia-Associated Transcription Factor Interacts with PU.1 and c-Fos: Determination of Their Subcellular Localization. Biochemical and Biophysical Research Communications. 1999;254(2):384–7.
17. Kalderon D, Roberts BL, Richardson WD, Smith AE. A short amino acid sequence able to specify nuclear location. Cell. 1984;39(3 Pt 2):499-509.
18. Kimura M, Imamoto N. Biological significance of the importin-beta family-dependent nucleocytoplasmic transport pathways. Traffic. 2014;15(7):727-48.
19. Strom AC, Weis K. Importin-beta-like nuclear transport receptors. Genome Biology. 2001;2(6)
20. Groves MR, Hanlon N, Turowski P, Hemmings BA, Barford D. The structure of the protein phosphatase 2A PR65/A subunit reveals the conformation of its 15 tandemly repeated HEAT motifs. Cell. 1999;96(1):99-110.
21. Strambio-De-Castillia C, Niepel M, Rout MP. The nuclear pore complex: bridging nuclear transport and gene regulation. Nature Reviews Molecular cell biology. 2010;11(7):490-501.
22. Kraft C, Peter M, Hofmann K. Selective autophagy: ubiquitin-mediated recognition and beyond. Nature Cell Biology. 2010;12(9):836-41.

23. Roczniak-Ferguson A, Petit CS, Froehlich F, Qian S, Ky J, Angarola B, et al. The transcription factor TFEB links mTORC1 signaling to transcriptional control of lysosome homeostasis. Science Signaling. 2012;5(228).
24. Martina JA, Chen Y, Gucek M, Puertollano R. MTORC1 functions as a transcriptional regulator of autophagy by preventing nuclear transport of TFEB. Autophagy. 2012;8(6):903-14.
25. Settembre C, Zoncu R, Medina DL, Vetrini F, Erdin S, Erdin S, et al. A lysosome-to-nucleus signalling mechanism senses and regulates the lysosome via mTOR and TFEB. The EMBO Journal. 2012;31(5):1095-108.
26. Sorokin AV, Kim ER, Ovchinnikov LP. Proteasome system of protein degradation and processing. Biochemistry Biokhimiia. 2009;74(13):1411-42.
27. Nguyen LK, Kolch W, Kholodenko BN. When ubiquitination meets phosphorylation: a systems biology perspective of EGFR/MAPK signalling. Cell Communication and Signaling : CCS. 2013;11:52.
28. Takebayashi K, Chida K, Tsukamoto I, Morii E, Munakata H, Arnheiter H, et al. The recessive phenotype displayed by a dominant negative microphthalmia-associated transcription factor mutant is a result of impaired nucleation potential. Molecular and Cellular Biology. 1996;16(3):1203-11.
29. Goodall J, Carreira S, Denat L, Kobi D, Davidson I, Nuciforo P, et al. Brn-2 represses microphthalmia-associated transcription factor expression and marks a distinct subpopulation of microphthalmia-associated transcription factor-negative melanoma cells. Cancer Research. 2008;68(19):7788-94.
30. Ploper D, Taelman VF, Robert L, Perez BS, Titz B, Chen HW, et al. MITF drives endolysosomal biogenesis and potentiates Wnt signaling in melanoma cells. Proceedings of the National Academy of Sciences of the United States of America. 2015;112(5):E420-9.
31. Kirkin V, Lamark T, Sou YS, Bjorkoy G, Nunn JL, Bruun JA, et al. A role for NBR1 in autophagosomal degradation of ubiquitinated substrates. Molecular Cell. 2009;33(4):505-16.
32. Park C, Cuervo AM. Selective autophagy: talking with the UPS. Cell Biochemistry and Biophysics. 2013;67(1):3-13.
33. Watanabe-Asano T, Kuma A, Mizushima N. Cycloheximide inhibits starvation-induced autophagy through mTORC1 activation. Biochemical and Biophysical Research Communications. 2014;445(2):334-9.
34. Miller AJ, Levy C, Davis IJ, Razin E, Fisher DE. Sumoylation of MITF and its related family members TFE3 and TFEB. The Journal of Biological Chemistry. 2005;280(1):146-55.
35. Murakami H, Arnheiter H. Sumoylation modulates transcriptional activity of MITF in a promoter-specific manner. Pigment cell research / sponsored by the European Society for Pigment Cell Research and the International Pigment Cell Society. 2005;18(4):265-77.
36. Miesenbock G, De Angelis DA, Rothman JE. Visualizing secretion and synaptic transmission with pH-sensitive green fluorescent proteins. Nature. 1998;394(6689):192-5.

Supplementary

Mutagenesis primers

Table 4. Primers used to produce MITF mutations.

Construct	Forward	Reverse	TA
258X	CCGGAAGTTGTAGCGGGAACAGC	ATGTAGTCCACAGAGGCC	65
278X	GGAGCATGCGTAGCGGCACCTGC	AGCTTCTTCTGTCGGTTTTCAAGGTC	70
298X	GCATGGACTTTAGCTTATCCCATCCAC	GCTCTAGCCTGCATCTCC	63
316X	TCGGATCATCTAGCAAGAACCAG	TTCACCAGATCAGGCGAG	64
Del1-70	CCCAACAGCCCTATGGCT	AGCAAGGTAAGCTTGAGCTC	66
Del1-120	GATGACATCATCAGCCTG	AGCAAGGTAAGCTTGAGC	60
Del1-170	AGCAACTCCTGTCCAGCC	AGCAAGGTAAGCTTGAGC	63
Del1-220	AACGACCGCATTAAGGAG	AGCAAGGTAAGCTTGAGC	63
E318K	CATCAAGCAAAAACCAGTTCTTG	ATCCGATTCACCAGATCAG	61
369A	CATCCCCAGGGCGATGGGCTCCAACTTG	CTGTAGGCCGGGCTGCTC	69
281-290A	GCTGCTGCTGCTGCTCAGGCTAGAGCGCATGGAC	AGCAGCAGCAGCAGCGTGCCGGTTCGCATGCTC	70
L267/274281F	TGAGCATGCGAACCGGCACTTTCTGCTCAGAGTACAGGAG	AACTTCTTCTGTCGGTTTTCAAAGTCCTTAGCTCGTTGCTG	62
B4RA	GCTGCTTTTAACATAAACGACCGC	AGCAGCTTCAATCAAGTTGTGATTGTC	58

Confocal images in inverted black and white (white and black)

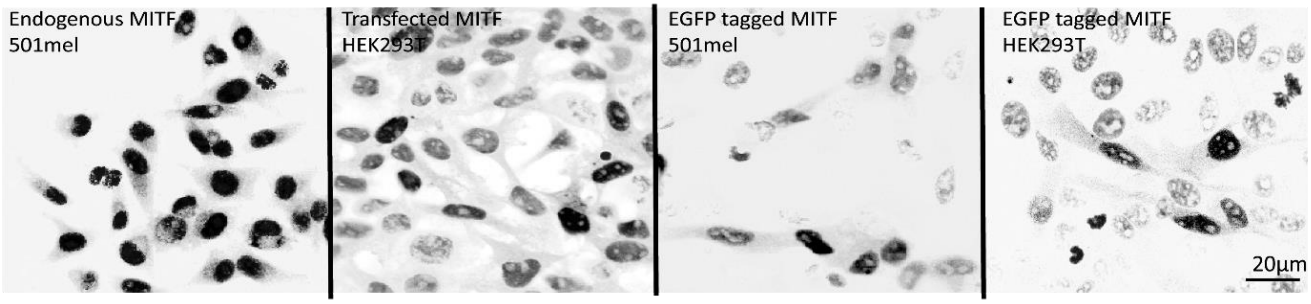

Figure 6. The MITF and GFP-MITF proteins are located in the nucleus. White and black version.

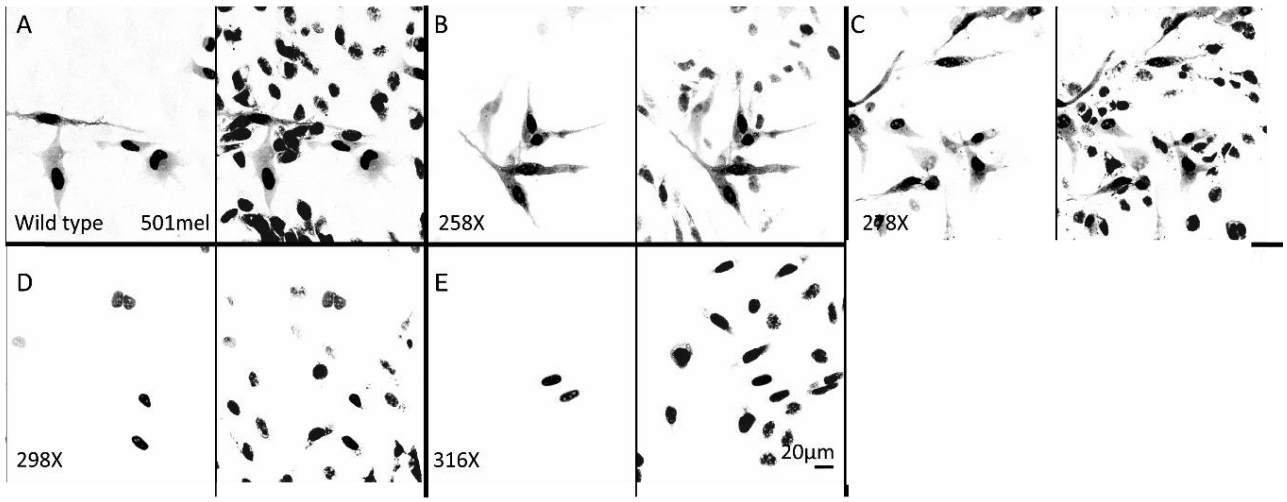

Figure 7. Subcellular localization of MITF C-terminal truncations. White and black version.

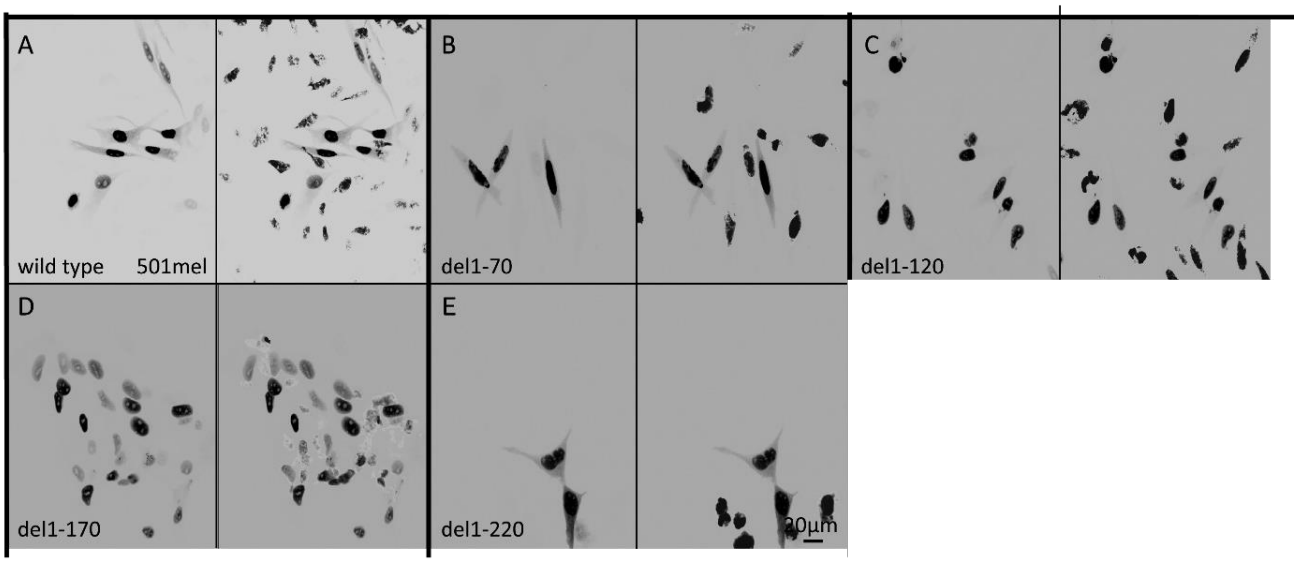

Figure 8. Subcellular localization of MITF N-terminal truncations. White and black version.

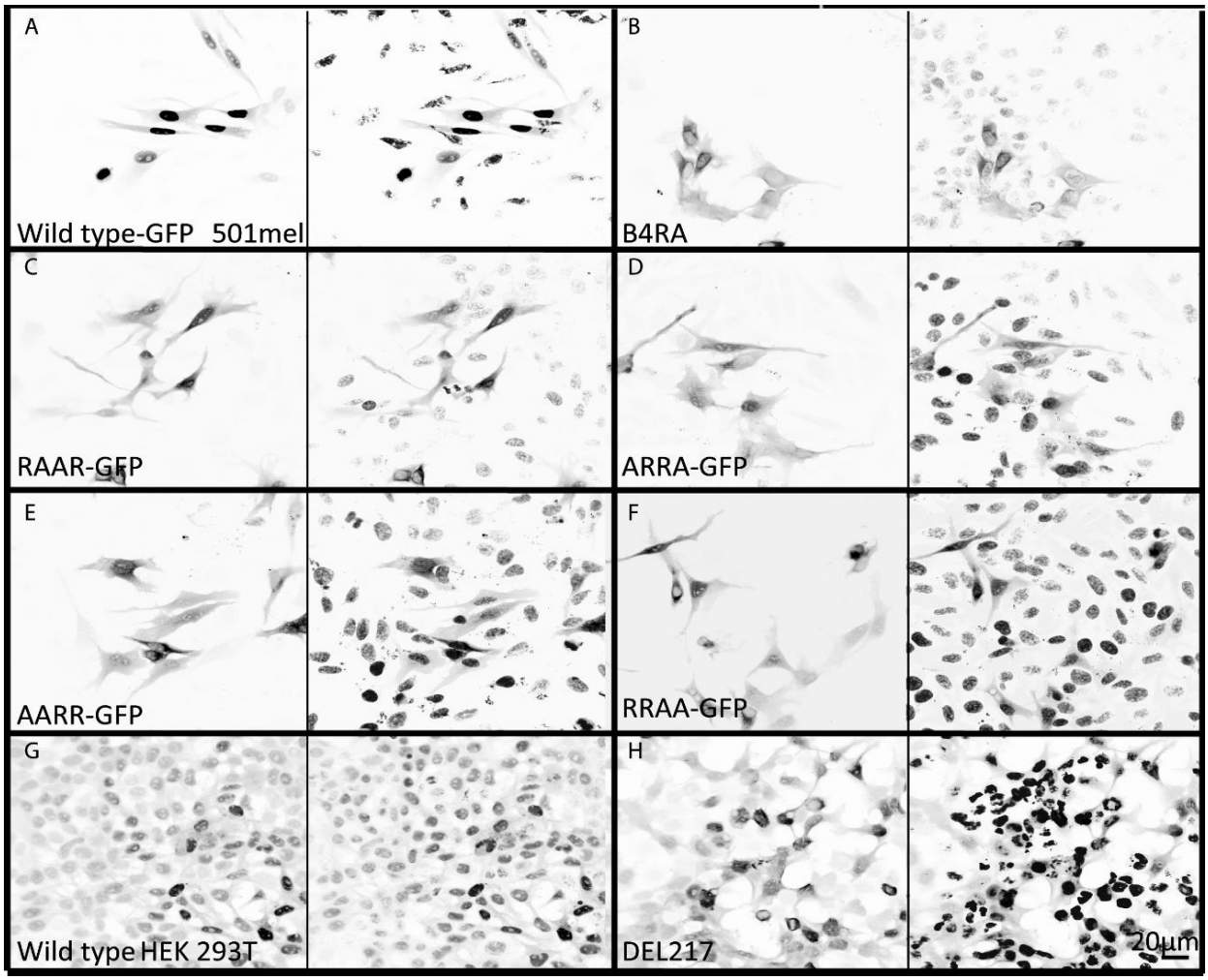

Figure 9. Effects of the basic domain on subcellular location of MITF: White and black version.

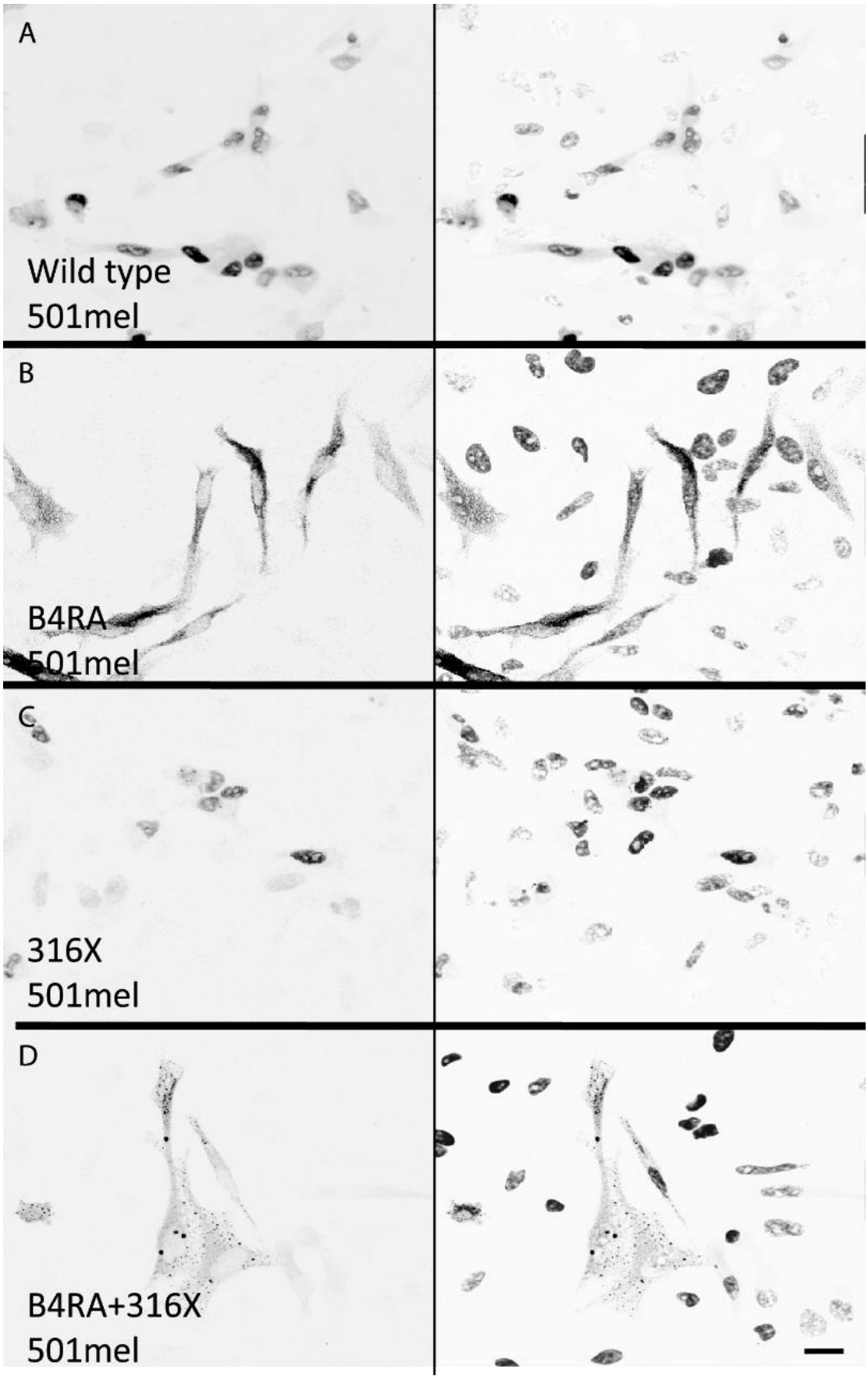

Figure 10. Effects of double mutations. White and black version.

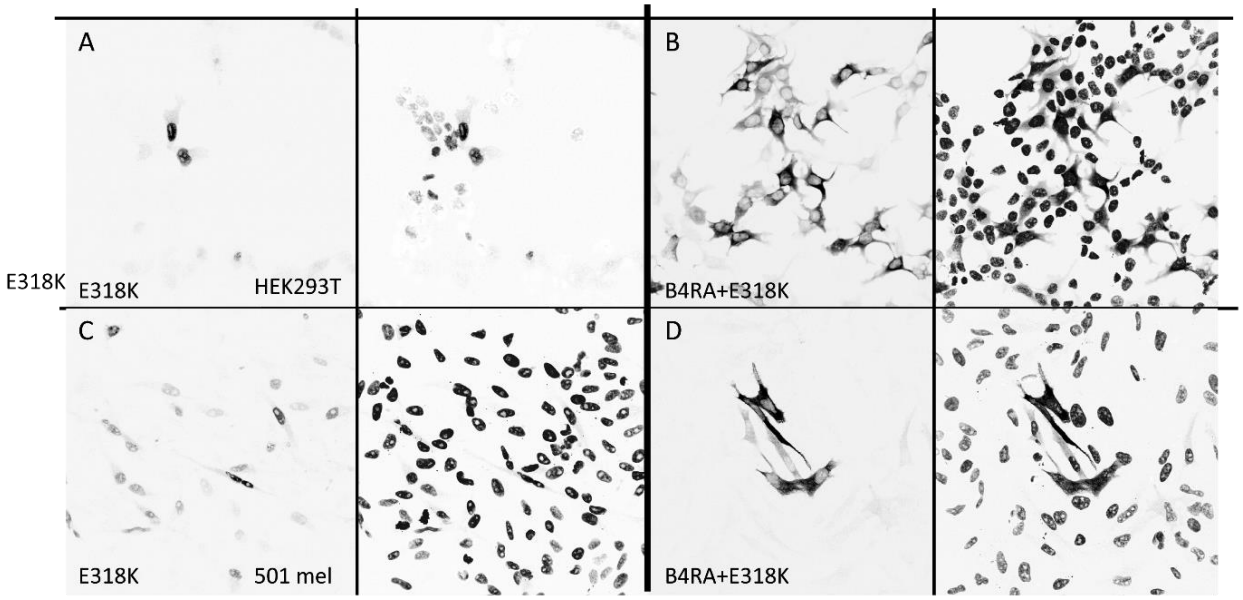

Figure 12. The E318K mutation does not replicate the 316X truncation phenotype. White and black version.

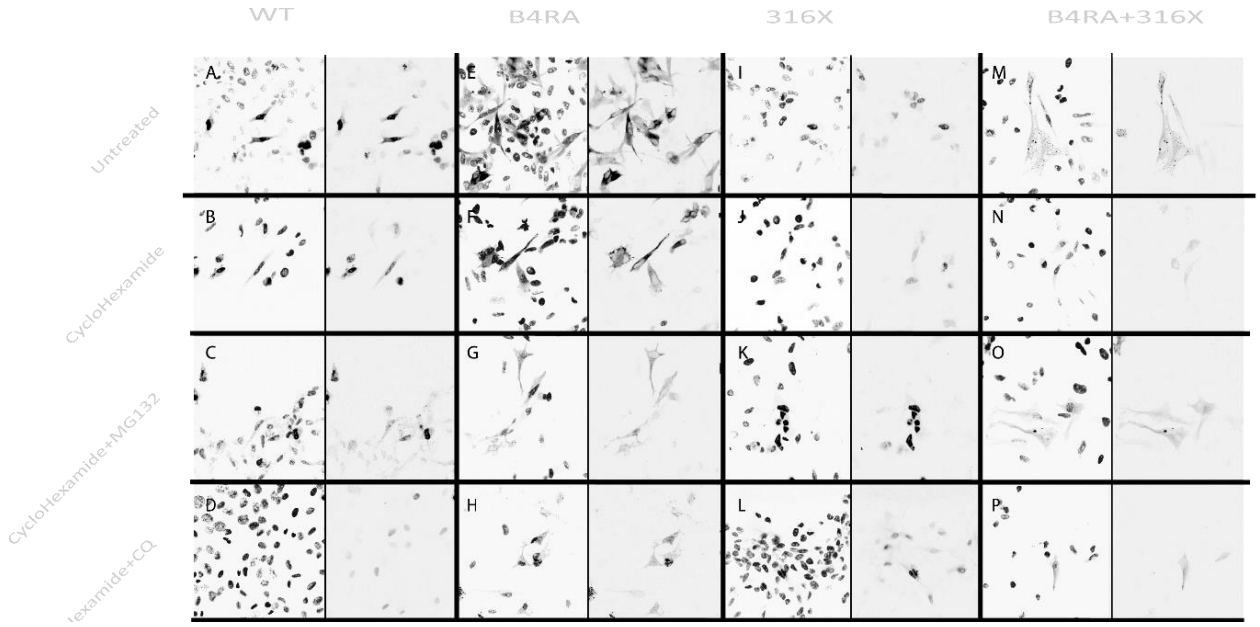

Figure 13 Effects of mutations on protein turnover. White and black version.